

T-1985

The Crystal Structure of Junitoite,  
 $\text{CaZn}_2\text{Si}_2\text{O}_7 \cdot \text{H}_2\text{O}$   
and  
The Crystallography and Crystal Chemistry of  
Zinc Silicates

by  
Robert D. Hamilton

ProQuest Number: 10796139

All rights reserved

INFORMATION TO ALL USERS

The quality of this reproduction is dependent upon the quality of the copy submitted.

In the unlikely event that the author did not send a complete manuscript and there are missing pages, these will be noted. Also, if material had to be removed, a note will indicate the deletion.



ProQuest 10796139

Published by ProQuest LLC (2019). Copyright of the Dissertation is held by the Author.

All rights reserved.

This work is protected against unauthorized copying under Title 17, United States Code  
Microform Edition © ProQuest LLC.

ProQuest LLC.  
789 East Eisenhower Parkway  
P.O. Box 1346  
Ann Arbor, MI 48106 – 1346

A Thesis submitted to the Faculty and the Board of Trustees of the Colorado School of Mines in partial fulfillment of the requirements for the degree of Doctor of Philosophy (Geology).

Signed: Robert D Hamilton  
Student

Golden, Colorado

Date: 8 May, 1978

Approved: [Signature]  
Thesis Advisor

[Signature]  
Head of Department

Golden, Colorado

Date: May 8, 1978

## ABSTRACT

Junitoite from the Christmas Mine, Arizona has the lattice parameters  $\underline{a}=12.510\text{\AA}$ ,  $\underline{b}=6.318\text{\AA}$ ,  $\underline{c}=8.561\text{\AA}$   $z=4$ , and occurs in space group  $Ama2$ . The structure was determined using Patterson and Fourier difference maps, then refined by least squares to  $R=.089$  for all 343 observed reflections.

The structure is based on continuous  $[\text{ZnO}_3]^{4-}$  chains extending along  $[010]$  connected by  $[\text{Si}_2\text{O}_7]^{6-}$  groups to form a continuous three dimensional tetrahedral network. Calcium is in octahedral coordination with five oxygens, each shared with two others cations, and one water molecule. The structure shows some similarities to clinohedrite and hardy-stonite but represents a new tetrahedral framework topology.

The dominant structural feature of all of the zinc silicates is the preference of zinc for tetrahedral coordination despite its large ionic radius. This preference is a result of two factors; the covalent nature of the zinc-oxygen bond, and the fact that during crystallization it is  $\text{Si}(\text{OH})_4$  groups and not oxygen atoms that are taken into coordination around the zinc ions.

There are approximately 25 natural and synthetic compounds which contain both zinc and silicon as essential constituents. Although diverse structurally the compounds

can be grouped into four categories based on structural and chemical similarities.

Approximately 40% of known zinc silicate structures are hemimorphic. Hemimorphic structures occur in two distinct groups; wurtzite derivative structures and structures which contain cations other than zinc and silicon with an ionic radius greater than  $0.8\text{\AA}$ .

Examination of the hemimorphic structures indicates that the occurrence of oversized zinc ions in tetrahedral coordination, the presence of nonequivalent Zn-O bonding, and the packing problems associated with incorporating large cations in a zincosilicate tetrahedral network, are all important in producing polar structures.

## Table of Contents

Acknowledgements.....	viii
Introduction.....	1
The Crystal Structure of Junitoite	
Introduction.....	2
Crystallography.....	3
Data Collection and Reduction.....	7
Structure Determination and Refinement.....	9
Description of the Structure.....	13
Discussion	
Si <sub>2</sub> O <sub>7</sub> Groups.....	19
Ca(O) <sub>5</sub> H <sub>2</sub> O Octahedrons.....	25
ZnO <sub>3</sub> Metachains.....	26
Cleavage.....	29
The Crystallography and Crystal Chemistry of Zinc Silicates	
Crystal Chemistry of Zinc.....	30
Zinc-Oxygen Coordination.....	30
Zinc-Oxygen Bonding.....	31
Zinc-(SiO <sub>4</sub> ) <sup>4-</sup> Coordination.....	34
Zinc Silicate Structures	
Classification.....	35
Group I-Simple Zinc Silicates.....	35
Group II-Wurtzite Derivative Structures.....	41
Group III-Complex Structures with Large Cations.....	42
Group IV-Complex Structures with Small Cations.....	46

Structural Patterns.....	47
Acentric Structures.....	49
Summary and Conclusions.....	54
Appendix. Observed and Calculated Structure	
Factors for Junitoite.....	56
References.....	63

## List of Figures and Tables

<u>Figure</u>		<u>Page</u>
1	Precession Photographs of Junitoite; hk0, hkl.....	5
2	Precession Photographs of Junitoite h0l, 0kl.....	6
3	Structure of Junitoite Viewed along $[010]$ .....	15
4	Structure of Junitoite Viewed along $[001]$ .....	16
5	Silicon-Bridging Oxygen Bond Length vs. Bridging angle.....	20
 <u>Table</u>		
1	Physical and Crystallographic Data for Junitoite.....	4
2	A Comparison of Junitoite Atomic Position Parameters for Space Groups Ama2 and Aba2.....	11
3	Atomic Positional Parameters for Junitoite.....	14
4	Junitoite Bond Lengths and Angles.....	21
5	Anion Coordination.....	24
6	Extension Factors and Optical Properties of $ZnO_3$ Chains.....	28
7	Classification of Zinc Silicates.....	36

### Acknowledgements

I would like to acknowledge the support and patient guidance provided by Dr. Joseph J. Finney during the course of this study. Dr. Sidney A. Williams provided the junitoite samples and the suggestion which instigated the study.

I would like to thank my committee members; Dr. David Olson, Dr. Samuel Romberger, Dr. Maynard Slaughter, Dr. David Snow, and Dr. Robert Witters, for their assistance in the preparation of this thesis.

The Colorado School of Mines provided financial assistance in many forms throughout this study.

## INTRODUCTION

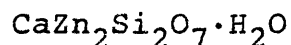
The purpose of this study was to determine the crystal structure of junitoite,  $\text{CaZn}_2\text{Si}_2\text{O}_7 \cdot \text{H}_2\text{O}$ , and, on the basis of this and other recently published structures, to examine in detail the crystal chemistry of zinc silicates.

All known crystal structures of both natural and synthetic compounds which contain both zinc and silicon as essential constituents have been examined and a systematic classification developed based on common chemical and structural features.

Two aspects of zinc silicates are of particular interest; the occurrence of zinc in tetrahedral coordination with oxygen despite its relatively large ionic radius, and the high percentage of acentric polar zinc silicate structures. These two zinc silicate features are examined in some detail.

Also included in this study is a synthesis of current information on the nature of the zinc oxygen bond as it is related to the coordination of zinc in these compounds.

## THE CRYSTAL STRUCTURE OF JUNITOITE,

INTRODUCTION

Junitoite was first described by S. A. Williams (1976) in material from the Christmas Mine, Gila County, Arizona. The Christmas Mine is a porphyry copper deposit with its production coming from skarns derived from the intrusion of a complex Laramide age diorite to granodiorite porphyry stock into Paleozoic carbonates (Perry, 1969). The skarns consist of garnet, wollastonite, and diopside with disseminated sphalerite and chalcopyrite. The junitoite occurs in portions of skarn which have undergone extensive retrograde metamorphism and oxidation. Junitoite is a secondary mineral associated with kinoite, apophyllite, smectite, calcite, and xonotlite.

The powder diffraction pattern of junitoite corresponds closely to that of an unnamed Ca-Zn-silicate phase obtained by Ito (1968) during the synthesis of Pb-Ca-Zn-silicates. Junitoite is named in honor of Dr. Jun Ito.

The junitoite used in this study was from Christmas Mine material provided by Dr. Williams. The sample contained junitoite as thin, colorless, rectangular plates approximately 2 mm x 2 mm x 0.05 mm nestled among larger euhedral apophyllite crystals. The apophyllite crystals were encrusting kinoite which was filling fractures in a

carbonate breccia.

#### CRYSTALLOGRAPHY

A summary of physical and crystallographic data for junitoite is presented in table 1. The space group reported by Williams was  $C_{2v}^{16}$ -Bbm2. The nonstandard orientation was chosen by Williams (1976) to establish a morphological correspondence between junitoite and hemimorphite. To facilitate calculations, Williams' a and b directions were interchanged (the orientation of the c axis being fixed by morphology) yielding the standard A-centered orientation, Ama2. This orientation will be used throughout the remainder of this paper.

Figures 2 and 3 show precession photographs of junitoite. Examination of the photographs reveals that in addition to the extinctions expected for Ama2 those hkl reflections for h odd are very weak indicating that heavy atoms occupy the 4a site 00z in which atoms are separated by  $\frac{1}{2}$  along a. There are only five very weak 0kl reflections for which k is odd, indicating the presence of a pseudo b-glide normal to a.

The unambiguous assignment of a noncentric space group is possible on the basis of the hemimorphic habit, asymmetric etch pits, and pyroelectric effect, all observed by Williams (1976).

Table 1. Junitoite, physical and crystallographic data

---

Formula:	$\text{CaZn}_2\text{Si}_2\text{O}_7 \cdot \text{H}_2\text{O}$	
Density:	calculated	$3.516 \text{ gm/cm}^3$
	observed	$3.5^\dagger \text{ gm/cm}^3$
Space group:	Ama2	
Unit cell:	$a_o$	$12.510(7)\text{\AA}$ $12.503\text{\AA}^\dagger$
	$b_o$	$6.318(3)\text{\AA}$ $6.309\text{\AA}^\dagger$
	$c_o$	$8.561(6)\text{\AA}$ $8.549\text{\AA}^\dagger$
	V	$676.6\text{\AA}^3$
	Z	4
Refractive Indices:	$\alpha$	$1.656^\dagger$
	$\beta$	$1.664^\dagger$ $2V_z = 86^\circ^\dagger$
	$\gamma$	$1.672^\dagger$
Optic Orientation:	X =	<u>b</u>
	Y =	<u>a</u>
	Z =	<u>c</u>

---

(n) number in parenthesis represents standard error

$^\dagger$  values taken from Williams (1976)

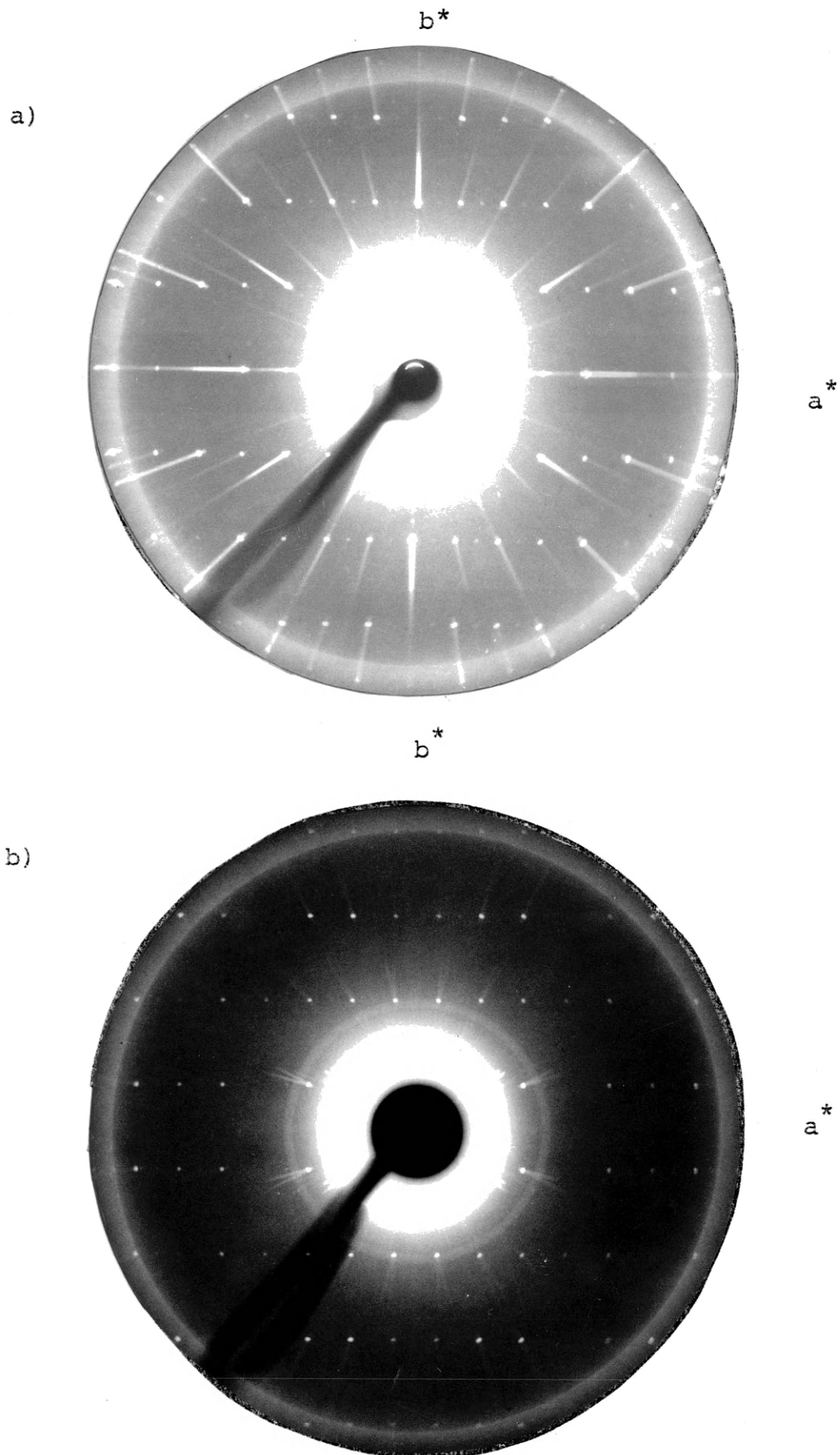


Figure 1. Precession photographs of junitoite,  $\text{MoK}_\alpha$  radiation. a)  $hk0$ , b)  $hkl$

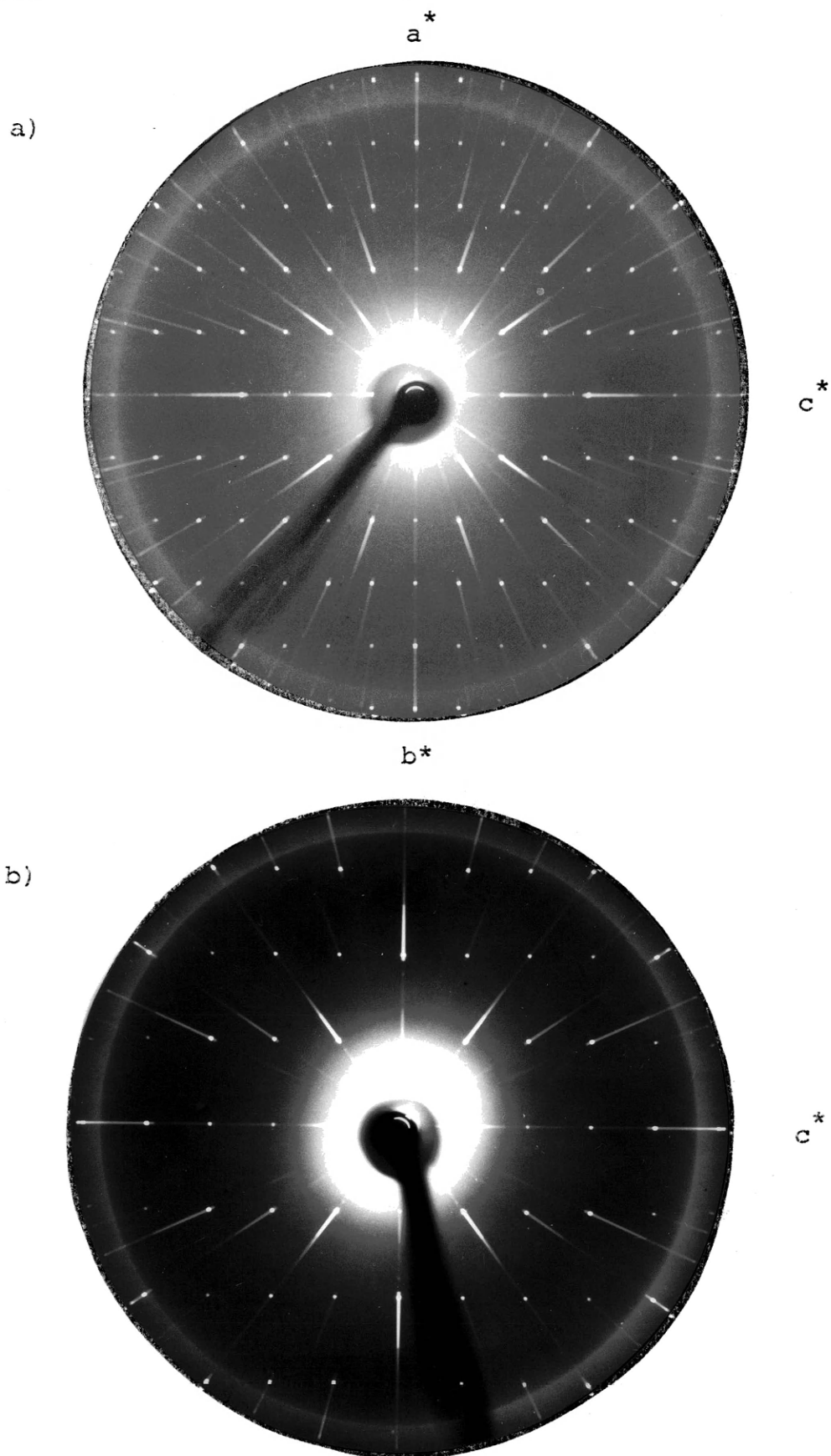


Figure 2. Precession photographs of junitoite, MoK $\alpha$  radiation. a) h0l, b) 0kl

DATA COLLECTION AND REDUCTION

Diffraction data were collected on a tabular crystal 0.1mm x 0.12mm x 0.05mm with the short dimension normal to {100}. The crystal was mounted on a glass fiber normal to {100}. Data were collected using a Syntex P1 automatic four-circle diffractometer equipped with a graphite monochromator employing MoK<sub>a</sub> radiation. A ω-2θ scan was used with a constant scan rate of 2° 2θ per minute with a 30 second background count at each end of the scan. A minimum scan range of ± 0.08° 2θ was employed. The intensities of 745 reflections with a maximum 2θ of 50° were measured in the positive octant.

Unit cell dimensions were determined by the least-squares refinement of 10 reflections scattered evenly throughout the reciprocal sphere. The cell parameters with their standard error are listed in table 1.

Data reduction was accomplished using the CUPBAR program written by C. A. Haultiwanger\*. Lorenz-polarization corrections were made assuming a monochromator which was 50% mosaic according to the equation

$$L_p = \frac{1}{\sin^2 2\theta_x} \left[ .5 \frac{\cos^2 2\theta_m + \cos^2 2\theta_x}{1 + \cos 2\theta_m} + .5 \frac{\cos 2\theta_m + \cos^2 2\theta_x}{1 + \cos^2 2\theta_m} \right]$$

where  $2\theta_x$  is the crystal diffraction angle and  $2\theta_m$  is the monochromator diffraction angle.

\*Department of Chemistry, University of Colorado

The calculated value for the linear absorption coefficient is  $83.8 \text{ cm}^{-1}$ , which, with an assumed mean spherical diameter of 0.01 cm, indicates that, if the crystal were spherical, satisfactory results might be obtained without absorption corrections. Because of the tabular shape of the crystal, general absorption corrections were calculated. Absorption corrections were calculated using the AGNOSTIC program of J.A. Ibers\* assuming a crystal described by six faces and employing the analytical option after de Muelenaer and Tompa (1965).

Standard deviations for the intensities were calculated using the method of Busing and Levy (1957) as modified by Cornfield, Doedens, and Ibers (1967). The equation used was

$$\sigma(I) = CT + 0.25(t_c/t_b)^2(B_1 + B_2) + p(I)^2$$

where CT is the total integrated peak counts obtained in time  $t_c$ ,  $B_1$  and  $B_2$  are the total background counts each obtained in time  $t_b$  and  $I = CT - 0.5(t_c/t_b)(B_1 + B_2)$ . A value of 0.03 was used for  $p$  which is described by Cornfield et al. (1967) as an ignorance factor which must be applied to prevent the assignment of unreasonably high weights to strong reflections during refinement. Due to the very large number of very weak reflections, resulting from the pseudo extinctions observed on the precession photographs, the entire data set containing all nonsystematically extinct reflections was used with all reflections being considered as observed and

\*Chemistry Department, Northwestern University

T-1985

weighted accordingly with  $w = 1/\sigma^2(F_{\text{Obs}}^2)$ .

#### STRUCTURE DETERMINATION AND REFINEMENT

Initial values for atomic coordinates were obtained by Patterson and Fourier methods. The Patterson and electron density maps were generated using NRC2 and NRC8 from the NRC Crystallographic Programs of Ahmed et al. (1967) with modifications for a DEC-10 computer.

The Patterson maps showed strong vectors in the sections with  $z=1/8, 1/4, 3/8, 1/2$ . From these maps it was possible to locate the zinc and calcium atoms. With these atoms approximately located an electron density difference map clearly showed the location of the silicon and one four-fold set of oxygens. A second difference map including these atoms allowed the location of the remaining oxygens.

Refinement of parameters was accomplished using ORFLS (Busing and Levy, 1962). Refinements were based on  $F$ , and intensities were weighted with  $w=1/\sigma^2(F_{\text{Obs}})^2$ . All structure factor calculations were based on neutral atom scattering factors from volume IV of the International Tables for X-ray Crystallography.

The structure was initially determined and refined in space group Ama2. The solution in this space group leads to having the eight zinc atoms divided ~~between~~ two four-fold

special positions separated by 0.496 z instead of being in a general eight-fold set as would be expected. With isotropic temperature factors the final discrepancy factor for unweighted intensities was  $R=.100$  and for weighted intensities  $R_w=.086$  where

$$R = \frac{\sum (|F|_{\text{obs}} - |F|_{\text{calc}})}{\sum W (|F|_{\text{obs}})}$$

$$R_w = \frac{(\sum W (F_{\text{obs}} - F_{\text{calc}})^2)^{\frac{1}{2}}}{(\sum W (F_o)^2)^{\frac{1}{2}}}$$

A comparison of  $F_{\text{obs}}$  and  $F_{\text{calc}}$  showed that  $F_{\text{calc}}$  for 0kl reflections for k odd were consistently larger than  $F_{\text{obs}}$  and that statistically all those reflections for k odd should be considered as unobserved. The only difference in systematic extinctions between Ama2 and Aba2 is the 0kl reflections. For Ama2, 0kl reflections are present when  $k+l = 2n$ , whereas Aba2 has reflections present where  $k=2n, l=2n$ . An attempt was made to refine the structure in Aba2, because the diffractometer data were more consistent with the space group Aba2 than Ama2 despite photographic evidence that Ama2 is the correct space group. It was possible to shift the entire structure intact to Aba2 by moving the origin so that

$$(x, y, z)_{\text{Aba2}} = (x - \frac{1}{4}, y - \frac{1}{4}, z)_{\text{Ama2}}$$

Upon shifting the origin the two four-fold zinc positions were transformed into a single eight-fold position, and two of the eight-fold oxygen sites were recombined into two new eight-fold sites. The remaining four-fold special positions transformed into equivalent positions in the new space group. Table 2 shows a comparison of atomic position in Ama2 and Aba2.

Table 2. A comparison of junitoite atomic position parameters for space groups Ama2 and Aba2.

atom		atom position in Ama2	Ama2 position shifted by $x-\frac{1}{4}, y-\frac{1}{4}, z$	refined atom position in Aba2
Ca	x	0.250*	0.000	0.000*
	y	0.246	0.006	0.000*
	z	0.112	0.112	0.114
Zn(1)	x	0.000*	0.750	
	y	0.000*	0.750	
	z	0.000*	0.000	0.753 0.751
Zn(2)	x	0.000*	0.750	0.000*
	y	0.000*	0.750	
	z	0.496	0.496	
Si	x	0.132	0.882	0.882
	y	0.735	0.485	0.483
	z	0.236	0.236	0.238
O(1)	x	0.044	0.794	0.794
	y	0.744	0.494	0.495
	z	0.376	0.376	0.378
O(2)	x	0.121	0.871	0.876
	y	0.531	0.281	0.288
	z	0.136	0.136	0.130
O(3)	x	0.126	0.876	0.976
	y	0.952	0.702	0.708
	z	0.125	0.125	0.134
O(4)	x	0.250*	0.000	0.000*
	y	0.772	0.522	0.500*
	z	0.327	0.327	0.328
H <sub>2</sub> O	x	0.250*	0.000	0.000*
	y	0.276	0.026	0.000*
	z	0.378	0.378	0.377

\*Coordinate values fixed by symmetry.

The space group change did not produce the anticipated changes in the R factor or the refined atomic positions. The final R factors for Aba2 were  $R=.097$  and  $R_w = .087$ . The final position parameters and temperature factors changed very little and it is impossible to tell from refinement of the diffractometer data which space group is correct. Although Aba2 is a preferable space group based on the degree of freedom it gives the zinc atoms, Ama2 produces less distortion of the coordination polyhedrons and gives a structure in which the site symmetry of the cations is more similar to other zinc silicates.

Electron density difference maps calculated with data which had no absorption correction and based on isotropic temperature factors showed a residual ripple around the heavy atoms on the order of 2 to 3  $e^-/\text{\AA}^3$ . Attempts to refine the uncorrected data with anisotropic temperature factors led to negative values for the anisotropic parameter  $u_{22}$  for the Ca, Zn, and Si atoms. This situation would not be unusual for uncorrected data from a tabular crystal if it were not for the fact that the crystal is tabular parallel to {100} and hence the  $u_{11}$  term should be the term to go negative. Attempts to refine absorption corrected data produced no change in the behavior of the temperature factors and resulted in a 2 percent increase in the final

R values. Attempts at site refinement and changing the space group to Aba2 produced no improvement. At this point there is no obvious reason for the negative anisotropic temperature factors but it is apparent that a new data set collected on a more nearly spherical crystal is necessary for a more accurate structure determination.

The final atomic position parameters with isotropic temperature factors are given in Table 3. There was a very high correlation between the z parameters of Zn(2), Ca, O(4), and H<sub>2</sub>O, a problem common in polar structures, and the refinement converged slowly. The fact that most of the electrons in the unit cell are associated with atoms in special positions made it difficult to locate accurately the light atoms in general positions, and caused a relatively high standard error for the light atom positions and bond lengths.

#### DESCRIPTION OF THE STRUCTURE

Figure 3 shows a polyhedral drawing of the structure of junitoite viewed along  $[010]$ . Figure 4 is a view along 001 of a portion of the structure bounded approximately by  $z=\frac{1}{4}$  and  $z=\frac{3}{4}$ . Zinc occurs in  $[\text{ZnO}_4]^{2-}$  tetrahedrons which share corners to form continuous  $[\text{ZnO}_3]_n^{4n-}$  chains along  $[010]$ . These chains are linked in the  $[001]$  directions by silicon tetrahedrons, each of which are members of an

Table 3. Positional parameters for junitoite

Position	Atom	X	Y	Z	$\beta$	
4a	2 0, 0, Z	Zn <sub>1</sub>		0.0000	1.23(10)*	
		Zn <sub>2</sub>		0.4963(14)	0.15(07)	
4b	m $\frac{1}{4}$ , Y, Z	Ca	0.2462(12)	0.1119(11)	0.40(12)	
		Ox <sub>4</sub>	0.7721(44)	0.3270(28)	0.46(36)	
		H <sub>2</sub> O	0.2746(64)	0.3785(45)	3.22(87)	
8c	1 X, Y, Z	Si	0.1316(03)	0.7348(11)	0.2359(12)	0.32(09)
		Ox <sub>1</sub>	0.0437(12)	0.7438(30)	0.3764(19)	0.72(25)
		Ox <sub>2</sub>	0.1213(15)	0.5314(29)	0.1360(31)	1.10(36)
		Ox <sub>3</sub>	0.1263(14)	0.9517(32)	0.1249(31)	1.21(34)

\* (nx) refers to the standard error of the last two digits.

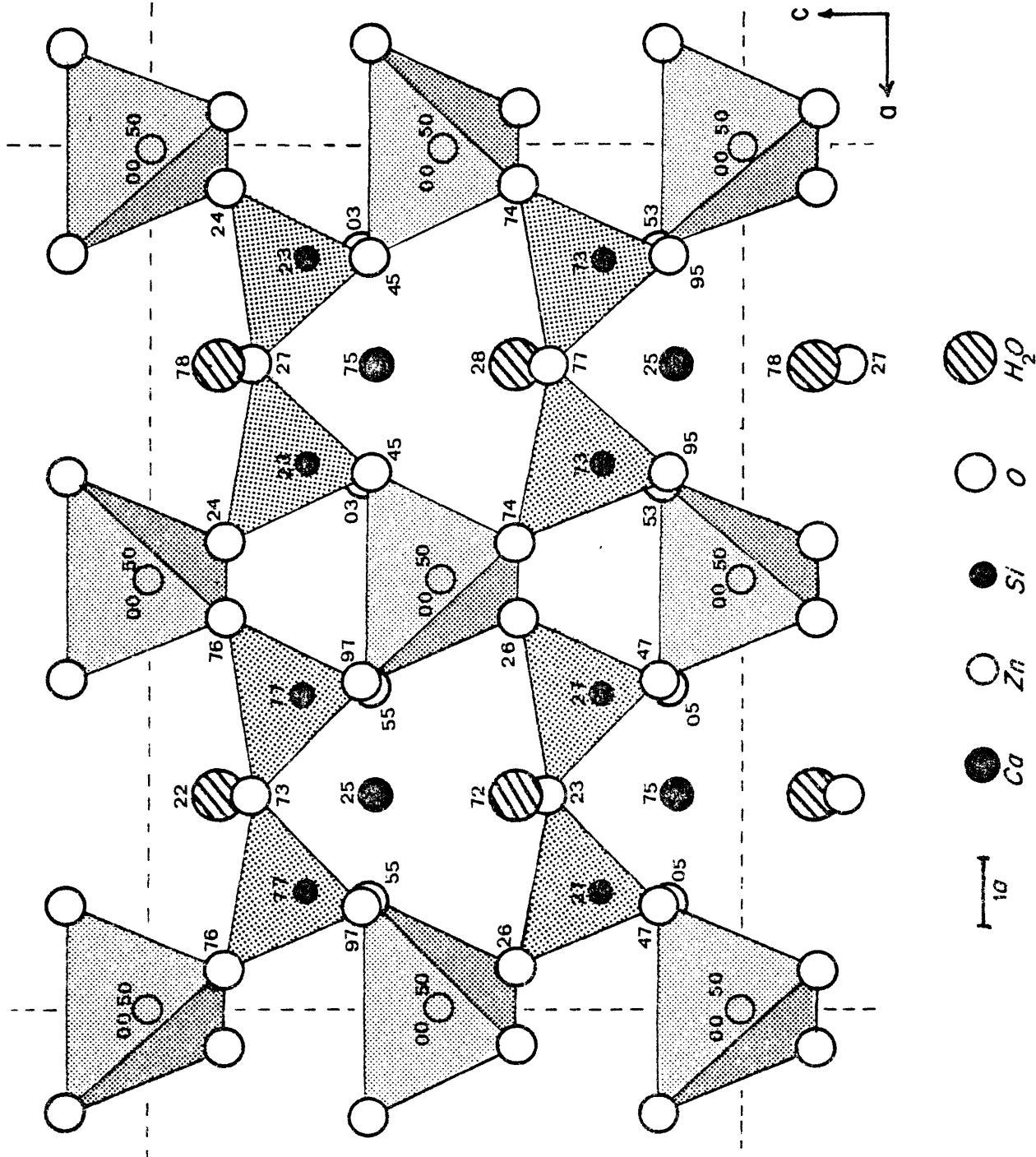


Figure 3. The structure of junitoite viewed along [010]. Numbers are the approximate Y coordinate of the atoms.

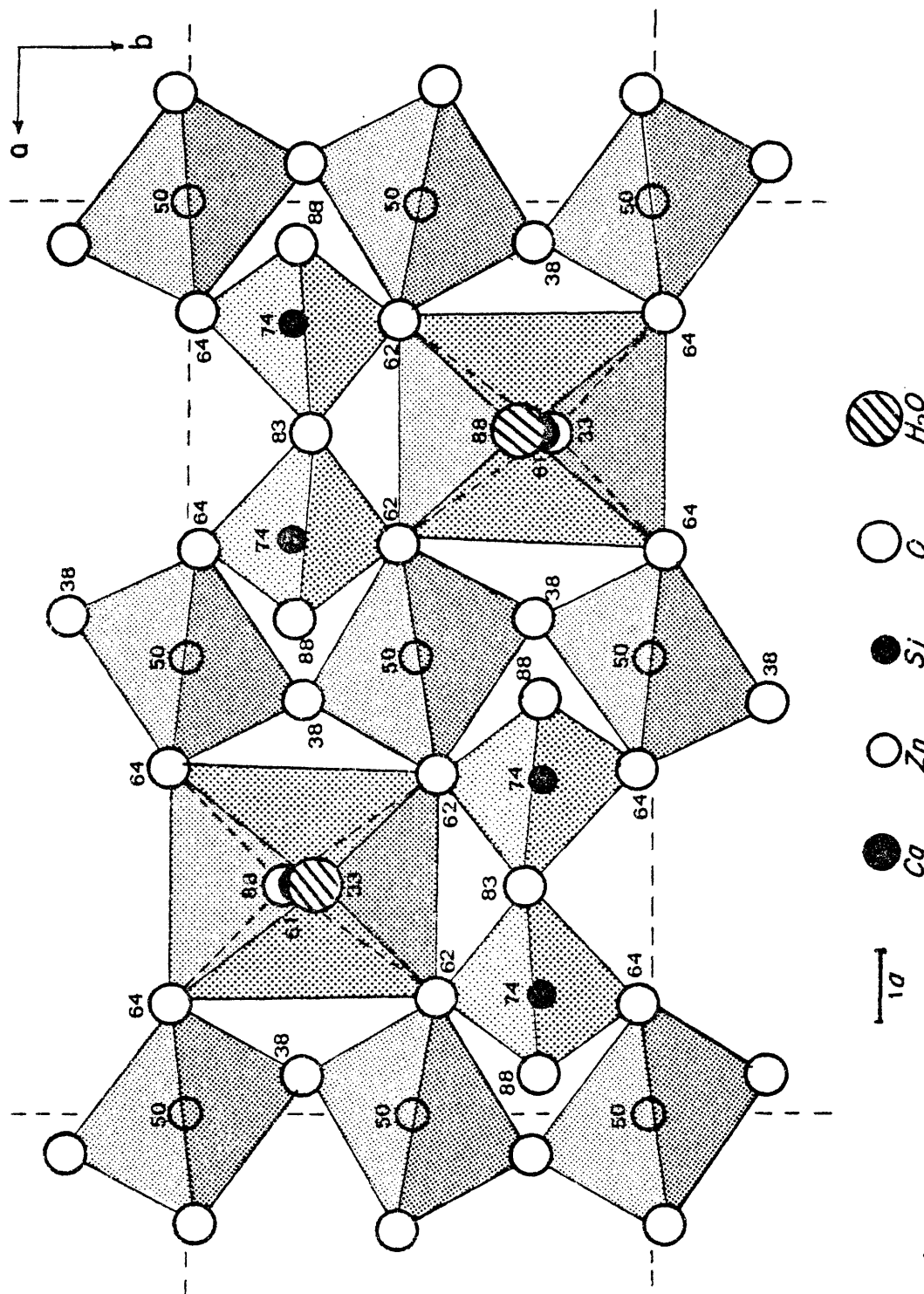


Figure 4. The structure of juninitoite viewed along [001]. Numbers are the approximate z coordinate of the atoms.

$[\text{Si}_2\text{O}_7]^{6-}$  disilicate group, to form zinc silicate sheets parallel to  $\{010\}$ . These sheets join through the bridging oxygen of the disilicate groups along  $a$  to form a three dimensional tetrahedral framework. Calcium occurs in distorted octahedrons with five oxygens, each of which is shared with two other cations, and a water molecule.

The two sets of zinc tetrahedrons are slightly distorted and not identical as can be seen from the bond lengths and angles given in Table 3. The average tetrahedral angle is close to ideal and the average Zn-O bond length of  $1.954\text{\AA}$  is identical to that found in hemimorphite (McDonald and Cruickshank, 1967) and similar to the  $1.95\text{\AA}$  average for all zinc silicates.

The Zn(1) and Zn(2) tetrahedrons are linked alternately through a shared corner oxygen, O(1), forming crenulated  $[\text{ZnO}_3]_n^{4n-}$  chains. These chains are different from the normal silicate chains in that two oxygens of each tetrahedron lie in a common basal plane and two lie in a common apical plane. Each unit cell contains two sets of these chains along  $[010]$  through the origin and related points. The sets have an opposite sense of crenulation as required by the space group symmetry.

The silicon tetrahedrons form isolated  $\text{Si}_2\text{O}_7^{6-}$  disilicate groups sharing a common oxygen, O(4). The disilicate groups are arranged across a mirror plane as they

are in hardystonite (Louisnathan, 1969) and hemimorphite. It may well be that the association of disilicate groups with mirror planes determines the space group of junitoite. In Aba2 the group falls astride a b-glide with a two-fold axis through the bridging oxygen, a configuration not found in any other mineral containing  $\text{Si}_2\text{O}_7$  groups.

The average Si-O bond length is consistent with other silicates and zinc silicates but the range of bond lengths is rather large and the 1.55 Å Si-O bond is unusually short. The Si-O-Si angle through the bridging oxygen is  $122.4^\circ$  which is smaller than the average of  $131.5^\circ$  for all disilicate groups in which the bridging oxygen is in three-fold coordination (Baur, 1971).

Calcium occurs in isolated, distorted  $\text{CaO}_5(\text{H}_2\text{O})^{8-}$  octahedrons which lie on a mirror plane. Four oxygens (O(2)x2, O(3)x2) lie in a plane approximately parallel to 001 and slightly above the calcium. The Ca-O bond lengths within the plane are 2.42 Å. Below the calcium on the mirror plane at a distance of 2.44 Å is a fifth oxygen, O(4), which is also the bridging oxygen of the disilicate group. Above the calcium at a distance of 2.29 Å is a water molecule. The Ca-O bond lengths fall at the maximum expected value based on ionic radius and observed bond lengths in other structures.

DISCUSSION

Si<sub>2</sub>O<sub>7</sub> groups. Although it is not unusual for silicon tetrahedrons to have a relatively short Si-O, bond on the order of 1.59Å, and a longer 1.67 to 1.69Å bond, the range and distribution of Si-O bonds in junitoite as shown in table 4 is unusual. Some, but not all, of the very large variation in Si-O bond lengths is undoubtedly related to the problems encountered in the refinement of the atomic positions as previously discussed.

The silicon bridging oxygen bond of 1.69Å is considerably longer than that found in either hardystonite (1.649Å) or hemimorphite (1.627Å). This much longer bond is, however, associated with a smaller Si-O-Si angle of 122.4° as compared with 138.5° and 150.3° for hardystonite and hemimorphite respectively. The plot of the cosecant of the Si-O-Si angle versus bridging oxygen bond length shown in Figure 5 shows a linear increase in bond length with decreasing bridging angle. This relation is expected because of increasing cation-cation repulsion with decreasing bridging angle. A similar relation between bond length and bridging angle has been observed in other silicates, but Baur (1970) did not find this relation in other minerals containing Si<sub>2</sub>O<sub>7</sub> disilicate groups.

In the case of the remaining terminal Si-O bond lengths the difference between the longer 1.67Å bond and the much shorter 1.55Å is more difficult to explain. Both bonds are

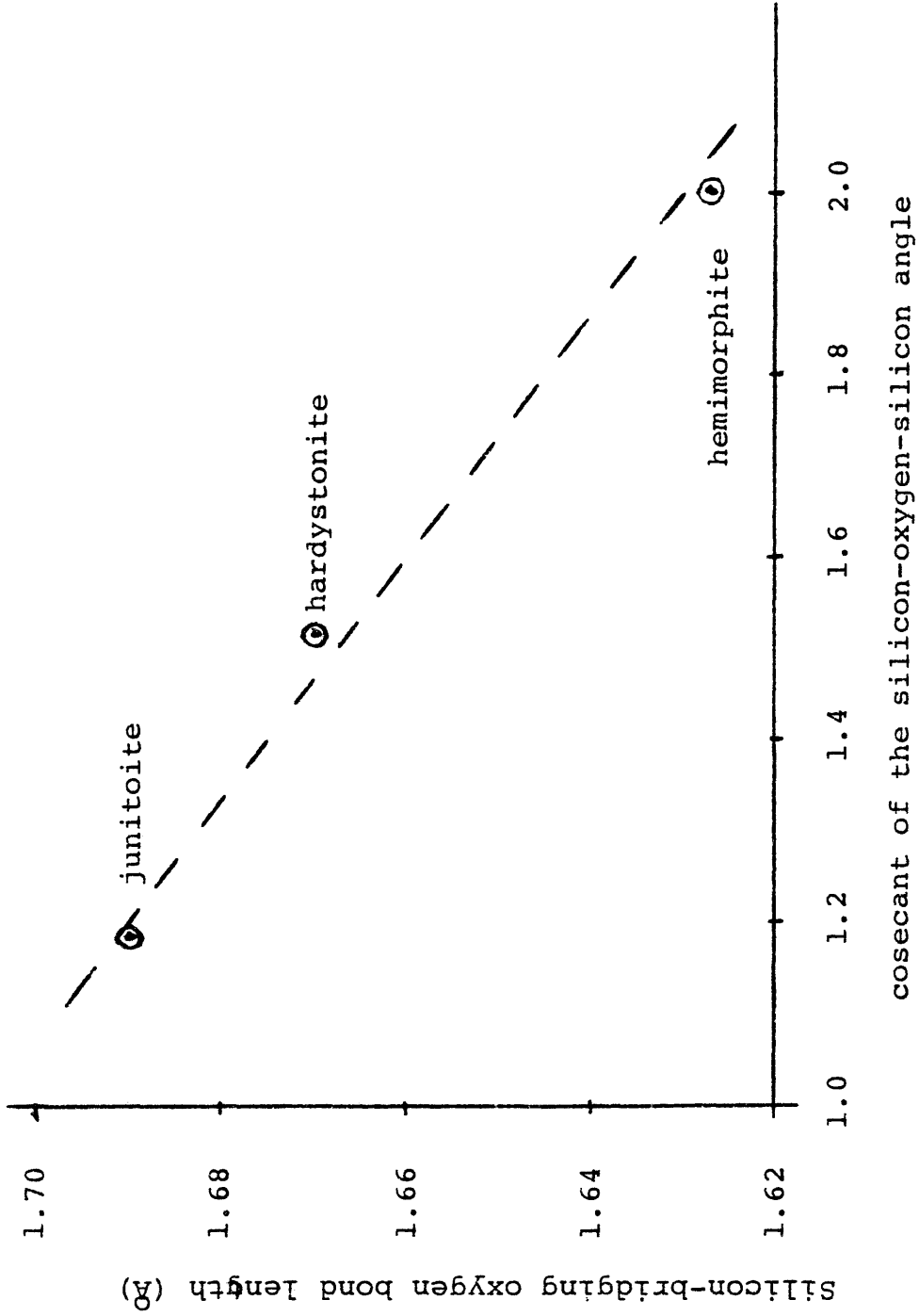


Figure 5 . Silicon-bridging oxygen bond length vs. bridging angle

Table 4. Junitoite bond lengths and angles

Zn(1)-tetrahedron							O-M-O angle
Zn-O(1)	2x	1.947(29) Å	O(1)	-O(1)		3.269(40) Å	114.5°
			O(3)	-O(3)	2x	3.000(48)	101.3°
					2x	3.252(48)	113.9°
	avg.	1.940					
			O(3)	-O(3)		3.049(53)	112.8°
					avg.	3.137	109.6
Zn(2)-tetrahedron							
Zn-O(1)	2x	1.994(35) Å	O(1)	-O(1)		3.417(40) Å	118.0°
			O(2)	-O(2)	2x	3.031(47)	100.7°
					2x	3.350(47)	116.7°
	avg.	1.968					
			O(2)	-O(2)		3.061(53)	104.4°
					avg.	3.206	109.7
Si-tetrahedron							
Si-O(1)		1.630(40) Å	O(1)	-O(2)		2.642(47) Å	112.3°
			O(2)	-O(3)		2.756(47)	113.4°
			O(3)	-O(4)		2.621(53)	104.2°
			O(4)	-O(3)		2.658(53)	111.3°
				-O(4)		2.753(58)	116.3°
	avg.	1.634					
			O(3)	-O(4)		2.584(58)	100.6°
Si-O(4)-Si angle							
					avg.	3.662	109.7

Table 4. continued

Ca-octahedron						O-M-O angle	
Ca-O(2)	2x	2.425(40) Å	O(2)	-O(2)		3.219(58) Å	83.2°
O(3)	2x	2.422(40)	O(2)	-O(3)	2x	3.664(53)	98.2°
O(4)		2.444(47)	O(2)	-O(4)	2x	3.502(58)	92.0°
H <sub>2</sub> O		2.291(70)	O(2)	-H <sub>2</sub> O	2x	3.082(78)	81.6°
			O(3)	-O(3)		3.094(53)	79.4
	avg.	2.405	O(3)	-O(4)	2x	3.605(58)	95.6
			O(3)	-H <sub>2</sub> O	2x	3.364(78)	91.0°
					avg.	3.396	90.0°
Hydrogen bonds							
H <sub>2</sub> O-O(2)		3.082 Å	O(2)	-H <sub>2</sub> O-O(2)			63.0°
O(3)		2.841	O(3)	-H <sub>2</sub> O-O(3)			54.8°
			O(2)	-H <sub>2</sub> O-O(3)			97.1°

to oxygens which have essentially identical cation coordinations (see Table 4) with the possible exception of hydrogen bonds.

Using the method outlined by Baur (1971) for estimating variations in Si-O bond lengths based on Pauling bond strength and assuming a full hydrogen bond to O(3) the minimum Si-O distance should be about  $1.62\text{\AA}$  and the maximum about  $1.66\text{\AA}$ . The longer calculated value agrees well with the observed value but the shorter values are considerably different.

An examination of the remaining cation-oxygen bond lengths associated with O(2) and O(3) (Table 5) reveals that the Ca-O bonds are identical while the Zn-O bonds vary greatly in length. The two zinc sites are clearly not equivalent based on the average Zn-O bond lengths and the tetrahedral angles. The shorter Si-O(2) bond is to an oxygen in the larger more highly distorted Zn(2) tetrahedron and the longer Si-O(3) bond to the smaller more regular Zn(1) tetrahedron. The variations in Si-O bond length are related to inequalities in the Zn-O bond strength. Because of the covalent nature of the Zn-O bond, Zn-O bond strength is a function of both electrostatic forces and the geometry of the  $\text{ZnO}_4$  tetrahedron. Geometric effects cannot be adequately accounted for in calculations of Baur's type. Brown (1977) pointed out similar problems in a number of complex structures and has made several suggestions on techniques for improving bond length predictions.

Table 5. Anion coordination

O(1)	-Zn(1)	1.947(29) Å	Zn(1)-O(1)-Zn(2)	106.6°
	Zn(2)	1.993(35)	Zn(1)-O(1)-Si	124.3°
	Si	1.630(40)	Zn(2)-O(1)-Si	126.4°
			avg.	119.1°
O(2)	-Ca	2.425(40)	Ca-O(2)-Si	127.5°
	Zn(2)	1.942(42)	Ca-O(2)-Zn(2)	113.0°
	Si	1.549(46)	Zn(2)-O(2)-Si	119.3°
			avg.	119.9°
O(3)	-Ca	2.422(40)	Ca-O(3)-Zn(1)	112.1°
	Zn(1)	1.932(38)	Ca-O(3)-Si	129.1°
	Si	1.669(47)	Zn(1)-O(3)-Si	118.5°
			avg.	120.0°
O(4)	-Ca	2.444(47)	Ca-O(4)-Si	2x 116.8°
	Si 2x	1.690(53)	Si-O(4)-Si	122.4°
			avg.	118.7°

CaO<sub>5</sub>H<sub>2</sub>O<sup>8-</sup> octahedrons. The average O-O distance in the calcium octahedron, 3.4 Å, is slightly larger than would be expected for oxygen in three-fold coordination and calcium in six-fold coordination. The O-O distances are long because of the articulated tetrahedral pairs which extend along the octahedral edges in the (001) plane as shown in Figure 4. The cation repulsion between adjacent tetrahedrons leads to a tendency to maximize the bridging angle between tetrahedrons which results in an increase in the length of the octahedral edge.

Megaw (1968) has shown that when octahedron edges are extended the octahedrally coordinated cation must be shifted away from the center toward either an edge or a vertex depending on the balance of the bonding forces. In junitoite the Ca<sup>2+</sup> ion is displaced toward the oxygen vertex (O(4)) and away from the H<sub>2</sub>O vertex because of the difference in Ca-O and Ca-H<sub>2</sub>O bond strength. The off center calcium ion in the calcium octahedron may be the primary source of the pyroelectric effect observed in junitoite as it is in the strongly piezo- and pyroelectric niobates and related compounds (Megaw, 1968).

Coordination around the water molecule is not favorable for hydrogen bonding. Although the distance to the potential acceptor of the hydrogen bond, O(3) at 2.84 Å, is reasonable, the 54.8° O(3)-H<sub>2</sub>O-O(3) angle is unfavorable. The very

short  $2.25\text{\AA}$  Ca-H<sub>2</sub>O distance is also indicative of little or no hydrogen bonding.

$[\text{ZnO}_3]_n^{4-}$  metachains. Structurally, according to Zoltai (1960), junitoite can be considered to be a three dimensional nonterminated tetrahedral structure. It has a tetrahedral sharing coefficient of 2.375 which is greater than quartz and most common framework silicates (2.00) but less than hemimorphite (2.75) and willemite (3.00). High tetrahedral sharing coefficients are characteristic of zinc silicates. Junitoite has 3,4,6,8, and 10 membered tetrahedral rings.

When the silicon and zinc tetrahedrons are considered separately the continuous  $[\text{ZnO}_3]_n^{4-}$  metachains become an obvious structural feature. These chains are a common structural element in zinc silicates as they appear not only in junitoite but also in hemimorphite, willemite, clinohedrite, hodgkinsonite, and larsenite. In each, except for willemite, the repeat unit is two tetrahedrons but the repeat period is variable.

If all the tetrahedrons making up a chain were perfect and undistorted the maximum repeat length would be a multiple of the edge length of the tetrahedron. It is possible to compare the relative differences in tetrahedral distortion and articulation within chains by comparing the repeat period with the average tetrahedral edge. An "elongation factor"

(EF) for a chain may be calculated using the relation

$$EF=T/(L \cdot n)$$

where T is the repeat period, L is the average tetrahedral edge as expressed by the average tetrahedral oxygen-oxygen distance, and n is the number of tetrahedrons per repeat unit. When EF is less than 1.0 the chain is compressed either by kinking or selective shortening of tetrahedral edges. EF greater than 1.0 indicates a lengthening of tetrahedral edges in the direction of the chain.

The data in Table 6 for zinc silicates which contain  $[\text{ZnO}_3]_n^{4-}$  chains shows that stretched chains ( $EF > 1.0$ ) are in the minority. In comparison to the range of values for zinc silicates the elongation factors for pyroxenes and pyroxenoids all fall between .92 and .99, indicating slightly compressed chains with minimal distortion. EF values that differ greatly from 1.0 are not favored in  $[\text{SiO}_3]_n^{2-}$  meta-chains because of the very stable tetrahedral configuration of silicon and oxygen. In  $\text{ZnO}_4$  tetrahedrons the cation is much too large, the metal oxygen bond weaker and the covalent bonding is not as important, hence the zinc tetrahedrons are much easier to distort.

Optically, structures with compressed chains have the Z index of refraction close, or parallel, to the length of the chain and those with stretched chains like junitoite have Z normal or nearly normal to the chains.

Table 6. Extension factors and optical properties of zinc silicates with  $ZnO_3$  chains.

	space group	chain direct	E.F.	optic orient
larsenite* $PbZnSiO_4$	$Pna2_1$	$[001]$	.80	$z=c$
hemimorphite $Zn_4Si_2O_7(OH)_2 \cdot H_2O$	$Imm2$	$[001]$	.80	$z=c$
hodgkinsonite $MnZnSiO_4(OH)_2$	$P2_1/a$	$[001]$	.91	$z \wedge c$ $38^\circ$
willemite $Zn_2SiO_4$	$R\bar{3}$	$[0001]$	.96	uniaxial positive
junitoite $CaZn_2Si_2O_7 \cdot H_2O$	$Ama2$	$[010]$	1.07	$z=c$
clinohedrite $CaZnSiO_4 \cdot H_2O$	$Cc$	$[10\bar{1}]$	1.09	$y \wedge c$ $-28^\circ$

\*See Table 7, page 36 for references.

Cleavage. Hodgkinsonite, clinohedrite, and hardystonite all have been described as having distinct zinc silicate sheets; their cleavage parallel to the proposed sheets supports the validity of this description. Junitoite has identifiable zinc silicate sheets parallel to both (100) and (010). The  $[\text{ZnO}_3]_n^{4-}$  chains lie in the (100) plane and are linked by silicon tetrahedrons to form sheets parallel to (100) similar to those in the other zinc silicates. There is, however, only poor cleavage parallel to these sheets indicating that they are not structurally important. These sheets are weak because of the elongation of the zinc meta-chains and the need to break Si-O bonds to cleave parallel to them. The  $\text{Si}_2\text{O}_7$  groups lie parallel to (010), a plane of good cleavage and form less obvious zinc silicate sheets parallel to (010).

THE CRYSTALLOGRAPHY AND CRYSTAL CHEMISTRY  
OF ZINC SILICATES

CRYSTAL CHEMISTRY OF ZINC

Zinc-Oxygen Coordination. Zinc is known to occur in four-, five-, and six-fold coordination, but in silicates zinc is most frequently observed in tetrahedral coordination. This coordination is surprising considering the ionic radius of  $\text{Zn}^{2+}$  is  $0.74\text{\AA}$  falling between the radii of  $\text{Mg}^{2+}$  ( $0.66\text{\AA}$ ) and  $\text{Fe}^{2+}$  ( $0.76\text{\AA}$ ), both of which occur predominately in octahedral coordination with oxygen.

The very strong tendency of zinc for tetrahedral coordination is evidenced by its geochemical distribution. With a size and charge comparable to magnesium and iron, zinc should be observed concentrated in the mafic silicates such as olivine, pyroxenes, amphiboles, and garnets. As a rule, however, these minerals are very low in zinc because the zinc generally will not enter the octahedral sites occupied by the iron and magnesium. Because of zinc's large size and low charge relative to silicon it does not substitute for silicon in tetrahedral sites and thus is effectively excluded from the common silicate minerals.

Willemite,  $\text{Zn}_2\text{SiO}_4$ , has a formula similar to olivine,  $(\text{Mg,Fe})_2\text{SiO}_4$ , but has a different structure based on a tetrahedral coordination of zinc.

Many zinc spinels (Brehler, 1969), both natural and synthetic have been studied and the great majority of them are normal spinels with zinc in the tetrahedral sites (ex. gahnite,  $\text{ZnAl}_2\text{O}_4$ ; franklinite,  $\text{ZnFe}_2\text{O}_4$ ; hetaerolite,  $\text{ZnMn}_2\text{O}_4$ ). Inverse zinc spinels occur only when there is a small highly charged cation present to compete with the zinc for the tetrahedral sites (ex.  $\text{TiZn}_2\text{O}_4$ ,  $\text{SnZn}_2\text{O}_4$ ).

In tetrahedral structures without silicon, i.e. phosphates, vanadates, arsenates, and sulfates, zinc shows less of a tendency for tetrahedral coordination and may be found in octahedral coordination, or both tetrahedral and octahedral coordination within the same structure.

The tendency for tetrahedral coordination results in the crystal chemical behavior of zinc being very similar to beryllium despite their difference in size ( $\text{Be}^{2+}$  0.31Å). Examples of some isostructural or nearly isostructural beryllium and zinc minerals are bromelite ( $\text{BeO}$ ) and zincite ( $\text{ZnO}$ ), phenacite ( $\text{Be}_2\text{SiO}_4$ ) and willemite ( $\text{Zn}_2\text{SiO}_4$ ), bertrandite ( $\text{Be}_4\text{Si}_2\text{O}_7(\text{OH})_2$ ) and hemimorphite ( $\text{Zn}_4\text{Si}_2\text{O}_7 \cdot \text{H}_2\text{O}$ ), and euclase ( $\text{BeAlSiO}_4(\text{OH})$ ) and clinohedrite ( $\text{CaZnSiO}_4 \cdot \text{H}_2\text{O}$ ). It should be noted that the size difference between zinc and beryllium is so large that there is no solid solution between isostructural minerals.

Zinc-Oxygen Bonding. The nature of the Zn-O bond has been a subject of considerable discussion. Based on electronegativity (Pauling, 1960) the Zn-O bond is 47% covalent in character and several arguments have been advanced supporting the existence of an even higher degree of covalency.

The average Zn-O bond length in zinc silicates is  $1.95\text{\AA}$ , which is much shorter than the  $2.10\text{\AA}$  sum of the ionic radii of three-fold coordinated oxygen,  $1.36\text{\AA}$ , and tetrahedrally coordinated  $\text{Zn}^{2+}$ ,  $0.74\text{\AA}$ . Louisnathan (1969) concludes that the short Zn-O distance is a positive indication of the strongly covalent nature of the Zn-O bond. He points out that the average Zn-O bond in hardystonite ( $1.936\text{\AA}$ ) compares well with the "expected" covalent bond length based on the shortest Zn-Zn distance observed in zinc metal ( $2.665\text{\AA}$ ) and the O-O distance in diatomic  $\text{O}_2$  ( $1.27\text{\AA}$ ). This correspondence must be fortuitous, however, because neither the Zn-Zn or O-O bond has any similarity to the Zn-O bond.

Pauling (1960) has assigned a tetrahedral covalent radius of  $1.31\text{\AA}$  to zinc based on interatomic distances in sphalerite and wurtzite. The fact that this radius is compatible with observed Zn-O bond lengths is often cited as evidence of the covalent nature of this bond.

Zinc with an atomic number of 30 has a neutral atom electron configuration of  $(\text{Ar}) 3d^{10} 4s^2$ . Between atomic number 28 and 29 the energy level of 3d electrons falls

below that of 4s electrons, hence ionization of zinc proceeds by removal of 4s electrons leaving a full complement of 10 3d electrons in the  $Zn^{2+}$  ion. The  $Zn^{2+}$  ion with a filled d shell can receive no crystal field stabilization energy and its coordination should not be affected by crystal field effects.

It has been suggested by Louisnathan (1969) and others that zinc forms covalent bonds through the formation of hybrid orbitals. The electronic structure of zinc ions rules out a covalent Zn-O bond in which zinc donates a portion of the bonding electrons, as is the case with the Si-O bond. Instead, zinc ions enter into a covalent bond with oxygen where each of the four tetrahedrally coordinated oxygen atoms donates an electron pair to the bond.

A possible source of additional tetrahedral stabilization is the formation of  $d\pi-p\pi$  bonds. This type of bonding was proposed and discussed extensively by Cruickshank (1961) in relation to the tetrahedral coordination of Si, P, S, and Cl. Although recent molecular orbital calculations show that  $d\pi-p\pi$  bonding is only of minor importance in the  $SiO_4^{4-}$  tetrahedron (Tossell, 1975), structural evidence suggests that this bonding mechanism may have some importance in the other tetrahedral groups mentioned. The formation of  $\pi$  bonds

between zinc and oxygen could explain the fact that observed Zn-O bond lengths are consistently shorter than predicted.

Zn-(SiO<sub>4</sub>)<sup>4-</sup> Coordination. The existence of a highly covalent Zn-O bond is the most frequently cited explanation for the tetrahedral coordination of zinc with oxygen despite its large ionic radius. There is, however, an alternative explanation, which does not involve covalent bonding.

If SiO<sub>4</sub><sup>4-</sup> tetrahedra, rather than oxygen atoms, are taken as the coordinating unit around the zinc the reason for tetrahedral coordination becomes clear. The SiO<sub>4</sub><sup>4-</sup> tetrahedra have an effective spherical radius of about 2.9Å which gives a radius ratio of Zn<sup>2+</sup>/SiO<sub>4</sub><sup>4-</sup> of 0.25 well within the range favorable for tetrahedral coordination.

Viewing the coordination of zinc in terms of the larger SiO<sub>4</sub><sup>4-</sup> units also has a significance in terms of the actual processes involved in crystallization. A large majority of the natural zinc silicates are hydrous and form from aqueous solutions. It is known that silicon in solution does not exist as Si<sup>4+</sup> ions, but rather as monomeric Si(OH)<sub>4</sub> (Berner, 1971). If initial crystallization of zinc silicates from solution involves the linking of Si(OH)<sub>4</sub> species with either Zn<sup>2+</sup> ions or zinc aquo-ions then the tetrahedral coordination of zinc is readily explained without the need to invoke covalent bonding.

It seems likely that a combination of both covalent bonding and  $\text{SiO}_4^{4-}$  coordination are responsible for the predominance of tetrahedral coordination of zinc and oxygen in zinc silicates.

### ZINC SILICATE STRUCTURES

Classification. Considering only zinc silicate minerals there is no clear basis for the division of zinc silicates into groups. With the inclusion of synthetic compounds, however, there are some parallel structural and compositional trends which allow a rough grouping of zinc silicates into four different categories. The proposed categories and their members are shown in Table 7. The basis for the properties of each group and its members will be discussed individually.

Group I-Simple zinc silicates. This group contains anhydrous compounds containing only zinc and silicon as cations. Included in group I are several synthetic zinc silicates which are nearly isostructural with iron-magnesium amphiboles and pyroxenes, and the only silicates except for phyllosilicates with zinc in six-fold coordination.

$\text{Zn}_2\text{SiO}_4$  exists in five known polymorphic forms.  $\text{Zn}_2\text{SiO}_4$ -I, willemite, is isostructural with phenacite,  $\text{Be}_2\text{SiO}_4$ , and not olivine. Hang et al. (1970) refined the structure of willemite and described it as being formed

Table 7. Classification of Zinc Silicates

compound	space group	reference
I. Simple zinc Silicates		
willemite $Zn_2SiO_4$ (I)	$R\bar{3}$	Hang et al. (1970)
$Zn_2SiO_4$ (II)	$I\bar{4}2d$	Marumo and Syono (1971)
$Zn_2SiO_4$ (III, IV)	unk.	" " " "
$Zn_2SiO_4$ (V)	Imma	Syono et al. (1971)
$ZnSiO_3$ (O)	Pbca	Morimoto et al. (1975)
$ZnSiO_3$ (M)	$C2/c$	" " "
$ZnMgSi_2O_6$	Pbca	" " "
II. Wurtzite derivative structures		
zincite ZnO	$P6_3mc$	Abrahams and Bernstein (1969)
$Li_2ZnSiO_4$ ( $\beta$ )	$Pmn2_1$	West (1975)
$Li_2ZnSiO_4$ ( $\gamma$ )	Pmnb	" "
$Na_2ZnSiO_4$ ( $\beta$ )	$Pmn2_1$	" "
III. Complex structures with large cations		
$Na_2ZnSi_2O_6$	Fdd2	Belokoneva et al. (1970)
$Na_2ZnSi_3O_8$	$P2_1$	Hesse et al. (1977)
larsenite $PbZnSiO_4$	$Pna2_1$	Prewitt et al. (1967)
esperite $Ca_3Pb(ZnSiO_4)_4$	$P2_1/n$	Moore and Ribbe (1965)
hardystonite $Ca_2ZnSi_2O_7$	$P\bar{4}2_1m$	Louisnathan (1969)

Table 7. Continued

compound	space group	reference
III. Continued		
clinochredrite $\text{CaZnSiO}_4 \cdot \text{H}_2\text{O}$	Cc	Venetopoulos and Rentzepieris (1976)
junitoite $\text{CaZn}_2\text{Si}_2\text{O}_7 \cdot \text{H}_2\text{O}$	Ama2	this paper
hemimorphite $\text{Zn}_4\text{Si}_2\text{O}_7(\text{OH})_2 \cdot \text{H}_2\text{O}$	Imm2	McDonald and Cruichshank (1967)
IV. Complex structures with small cations		
hodgkinsonite $\text{Zn}_2\text{MnSiO}_4(\text{OH})_2$	$P2_1/a$	Rentzeperis (1963).
gerstmannite $(\text{Mn}, \text{Mg})\text{Mg}(\text{OH})_2(\text{ZnSiO}_4)$	Bbcm	Moore and Araki (1977a)
holdenite $(\text{Mn}, \text{Mg})_6\text{Zn}_3(\text{OH})_8(\text{AsO}_4)_2\text{SiO}_4$	Abma	Moore and Araki (1977b)
mcgovernite $\text{Mn}_9\text{Mg}_4\text{Zn}_2\text{As}_2\text{Si}_2\text{O}_{17}(\text{OH})_{14}$	$R\bar{3}2/c$	Wuensch (1960)
sauconite $\text{Na}_{0.33}\text{Zn}_3(\text{Si}, \text{Al})_4\text{O}_{10}(\text{OH})_2 \cdot 4\text{H}_2\text{O}$	?	Ross (1946)
hendricksite $\text{K}(\text{Zn}, \text{Mn})_3\text{AlSi}_3\text{O}_{10}(\text{OH})_2$	2/m	Fron del and Ito (1966)
zincsilite $\text{Zn}_3\text{Si}_4\text{O}_{10}(\text{OH})_2 \cdot n\text{H}_2\text{O}$	?	Smol'yaninova et al. (1961)

from  $\text{ZnO}_3$  metachains entwined about the  $3_1$  and  $3_2$  screw axis. These metachains are linked by isolated silicon tetrahedra to form a framework structure. The chains are formed by corner sharing  $\text{ZnO}_4$  tetrahedrons and are similar to the chains found in silicates but with a different articulation. Zn-O bond lengths average  $1.97\text{\AA}$ .

Willemite transforms to  $\text{Zn}_2\text{SiO}_4$ -II at about 30 kbars. Phase II is tetragonal,  $I\bar{4}2d$ , but still has zinc in tetrahedral coordination. The structure of phase II (Marumo and Syono, 1971) is based on an approximate body centered arrangement of oxygens with zinc occupying one of two types of tetrahedral sites and silicon the other. Phase II also contains  $\text{ZnO}_3$  chains, in this instance along  $[\bar{1}10]$ , which are linked by isolated silicon tetrahedra. The average Zn-O bond is  $1.98\text{\AA}$ . Muramo and Syono (1971) report an 8.8% decrease in cell volume with the I to II transition. This volume change is not accompanied by a coordination or bond length change and hence phase II is a very densely packed tetrahedral structure.

Phases III and IV exist between 70 and 150 kbars. The structures of these phases are unknown but from density changes they appear to retain zinc in tetrahedral coordination. Both phases are nonstoichiometric (Syono, et al., 1971).

Phase V which forms above 130 kbars is once again stoichiometric but now contains zinc in octahedral coordination (Syono et al., 1971). The structure of phase V is a modified spinel similar to that of  $\beta\text{-Mn}_2\text{GeO}_4$  and  $\beta\text{-Mg}_2\text{SiO}_4$  (Morimoto, et al., 1969). The beta spinel structure is an orthorhombic modification of a cubic spinel structure with a different arrangement of octahedral and tetrahedral sites. The structure is unusual in that the tetrahedral sites are links in pairs to form  $\text{M}_2^{\text{IV}}\text{O}_7$  elements which are isolated by edge and corner sharing octahedra. One of the oxygens is not bonded to any tetrahedral units and the structure may be represented by the formula  $\text{Zn}_4(\text{Si}_2\text{O}_7)\text{O}$ .

Experimental data indicates that, within the limits of the experiments, it is impossible to force  $\text{Zn}_2\text{SiO}_4$  into the olivine structure. The retention of zinc in tetrahedral coordination at pressures up to 130 kbars despite the marked increase in the packing emphasizes the unwillingness of zinc to assume octahedral coordination. The transformation to a beta-spinel phase is unusual for a compound with a phenacite structure. Most compounds with this structure transform directly to a cubic spinel structure at high pressures (Marumo and Syono, 1971). The failure of  $\text{Zn}_2\text{SiO}_4$  to assume a cubic spinel structure may be due to the large difference in the size of the two cations as compared to other phenacite structured compounds.

At high pressure it is possible to synthesize zinc analogues of both ortho- and clinopyroxenes (Syono, et al., 1971). The monoclinic form is stable only above 850°C and 30 kbars while the orthorhombic form is metastable at temperatures and pressures well below these values.

In monoclinic  $\text{ZnSiO}_3$  zinc in the M1 site is in a regular octahedral coordination with Zn-O bond lengths which range from 2.018Å to 2.333Å, with a mean of 2.145Å which is consistent with that observed for zinc in six-fold coordination (Brehler, 1969). Zinc in the M2 site is tetrahedrally coordinated with a mean Zn-O bond of 1.982Å. In orthorhombic  $\text{ZnSiO}_3$  the M1 zinc is also octahedrally coordinated with a mean Zn-O bond length of 2.128Å, but the M2 zinc is now also in octahedral coordination according to Morimoto et al. (1975). The coordination around the M2 site consists of four short Zn-O bonds ranging from 1.920Å to 2.046Å and two much longer bonds of 2.688Å and 2.955Å. The two long bonds are much longer than those normally observed for octahedral coordination, and the four short bonds are comparable to those found in tetrahedral coordination. It is therefore more accurate to describe the M2 site in the orthorhombic form as being one of distorted tetrahedral rather than octahedral coordination.

The tetrahedral coordination of the M2 site represents a marked departure from the normal pyroxene structure where the site is usually one of six- or eight-fold coordination.

Although it contains magnesium,  $\text{ZnMgSi}_2\text{O}_6$  can be logically included in this group because of its structural relation to the other pyroxene-like silicates. The structure of  $\text{ZnMgSi}_2\text{O}_6$  (Morimoto, et al., 1975) is intermediate between that of enstatite and orthorhombic  $\text{ZnSiO}_3$ . The zinc and magnesium atoms are partially ordered with 64% Zn in M2 sites and 36% in M1 sites. This ordering is to be expected if the M2 site in orthorhombic  $\text{ZnSiO}_3$  is considered to be tetrahedral instead of octahedral as described by Morimoto et al. (1975). The fact that the M2 sites are tetrahedral and not octahedral shows that these zinc silicates are only pseudopyroxenes and not true analogues of Fe, Mg-pyroxenes.

Group II-Wurtzite Derivative Structures. The organization of this group of structures is based on work by West (1975) concerning the synthesis and classification of  $\text{A}_2\text{BCO}_4$  tetrahedrally coordinated oxides where A=Li, Na; B=Be, Mg, Zn; and C=Si, Ge. All combinations of A, B, and C have not been synthesized but the structures of those that have can all be derived from the wurtzite structure. The wurtzite structure is based on hexagonal closest packing of anions with cations occupying all of one of the two sets of tetrahedrally coordinated voids.

Zincite,  $\text{ZnO}$ , (Abrahams and Bernstein, 1969) has a wurtzite structure and the remaining compounds in group II of the table have structures which may be derived from it. For this group zincite should be thought of as  $\text{Zn}_2\text{ZnZnO}_4$  and

then the remaining compounds can be derived by substitution of elements from the A, B, C lists above for zinc.

The wurtzite structure is polar with all of the apices of the occupied tetrahedral set oriented in the same direction along  $\underline{c}$  and opposite to the direction of the empty set. Zincite and all of its direct derivatives, which West (1975) calls  $\beta$  forms, are polar structures with all of one set of tetrahedral sites filled. It is possible to derive a polymorphic  $\gamma$ -phase for each  $\beta$ -phase by redistribution of the cations into both tetrahedral sites. This redistribution leads to a centric, nonpolar structure which contains shared tetrahedral edges between A cations and either B or C cations. In  $\gamma$ - $\text{Li}_2\text{ZnSiO}_4$  lithium and zinc tetrahedrons share edges because of their low charge relative to silicon. The  $\gamma$ -phase of  $\text{Na}_2\text{ZnSiO}_4$  does not exist and its failure to form can be attributed to the large radius of the  $\text{Na}^+$  ion. The  $\text{Na}^+$  ion is much too large for tetrahedral coordination and consequently distorts the tetrahedron which leads to an increase in the  $\text{Na}^+ - \text{Zn}^{2+}$  cation - cation repulsion. In the analogous system  $\text{Na}_2\text{BeSiO}_4$  both phases are present because the much smaller  $\text{Be}^{2+}$  ion reduces the strength of the cation - cation repulsion.

Group III-Complex Structures with Large Cations. All the compounds in this group have three features in common: all contain cations larger than zinc in five-fold or higher

coordination, they form three dimensional framework structures, and all but one is noncentric. With the exception of hemimorphite the compounds are lacking in hydroxyl water and, in contrast to the previous groups, a majority of the compounds in group III are minerals.

The two sodium members of this group are synthetic Heese et al., (1977) have determined the structure of  $\text{Na}_2\text{ZnSi}_3\text{O}_8$  and describe it as being related, but not identical, to that of sodic plagioclase. The tetrahedral framework is similar in topology and bond lengths to paracelsian with an ordering of the zinc. The  $\text{Na}^+$  ions fill cavities with an irregular seven- to eight-fold coordination. The mean Zn-O bond is  $1.95\text{\AA}$ , which is consistent with that found in the simpler compounds of the first two groups.

Belokoneva et al. (1970) determined that synthetic  $\text{Na}_2\text{ZnSi}_2\text{O}_6$  is isostructural with the mineral chkalovite,  $\text{Na}_2(\text{Zn}_2\text{Cd})\text{Si}_2\text{O}_6$ . The structure contains highly crenulated  $\text{SiO}_3$  chains which are linked by isolated  $\text{ZnO}_4$  tetrahedrons into a  $\text{ZnSiO}_6$  framework. The  $\text{Na}^+$  ions are in five-fold coordination with an average Na-O bond of  $2.45\text{\AA}$ . The mean Zn-O bond is  $1.92\text{\AA}$ , which is unusually short for zinc silicates. The framework structure of the two sodium zinc silicates is similar except for the longer four tetrahedral repeat distance found in the silicate chains of  $\text{Na}_2\text{ZnSi}_2\text{O}_6$ .

Larsenite  $\text{PbZnSiO}_4$  (Prewitt, et al., 1967) has a

frame built of five membered tetrahedral rings. Five tetrahedrons, three of zinc and two of silicon are linked into five membered rings lying in the (100) plane with all apices pointing in the same direction. The rings are linked by their apical oxygens along  $[001]$  to form a three dimensional network. One of the oxygens is shared only between one zinc and one silicon atom forming  $ZnSiO_7$  units with much shorter metal-oxygen bonds. The lead is in channels between the rings with three or four nearest neighbors in a very irregular coordination typical of lead.

Esperite (calcium larsenite)  $(Ca,Pb) ZnSiO_4$  has an unknown structure. According to Moore and Ribbe (1965) it has a subcell symmetry of  $P2_1/n$  with super lattice reflections originating from Pb-Ca ordering. The subcell dimensions for esperite show a relation to the dimensions of the larsenite cell. Preliminary structure calculations indicate that the structure is more closely related to beryllonite  $NaBePO_4$  than larsenite and is not a simple case of an ordered calcium-lead larsenite.

Hardystonite  $Ca_2ZnSi_2O_7$  (Louisnathan, 1969) is isostructural with melilite and is the only zinc silicate which has an exact aluminosilicate analogue, lawsonite. Hardystonite contains  $Si_2O_7$  disilicate groups which are joined by isolated  $ZnO_4$  tetrahedrons to form  $ZnSi_2O_7$  sheets normal to  $c$ . The calcium is in eight-fold coordination in distorted

square antiprisms between the zinc-silicate layers. The strong basal cleavage is a result of this layer-like structure. A lead analogue of hardystonite has been synthesized and is isostructural with hardstonite.

Clinohedrite  $\text{CaZnSiO}_4 \cdot \text{H}_2\text{O}$  (Venetopoulos and Rentzeperis, 1976) contains  $\text{ZnO}_4$  tetrahedrons linked to form continuous  $\text{ZnO}_3$  chains along  $[101]$ . The silicon tetrahedrons are isolated and the calcium ions are in octahedral coordination with four oxygens and two water molecules. The calcium octahedrons form edge sharing chains along  $[001]$ .

Junitoite  $\text{CaZn}_2\text{Si}_2\text{O}_7 \cdot \text{H}_2\text{O}$  has structural features common to both hardystonite and clinohedrite. Junitoite contains  $\text{ZnO}_3$  chains along  $[101]$  similar to those in clinohedrite. The chains are linked by  $\text{Si}_2\text{O}_7$  disilicate groups along  $[100]$  forming a three dimensional tetrahedral network. Calcium is in distorted octahedral coordination with five oxygens and one water molecule. The calcium octahedrons are isolated and not edge sharing as in clinohedrite.

Calcium zinc silicates have some structural elements in common but are all unique. The bond lengths of all calcium zinc silicates are consistent and similar to those found in other zinc silicates.

Hemimorphite  $\text{Zn}_4\text{Si}_2\text{O}_7(\text{OH})_2 \cdot \text{H}_2\text{O}$  could have been included in either group I or group IV based on its composition but because of its structure it has been placed in group III.

Hemimorphite is a three dimensional network of tetrahedrons formed by  $\text{ZnO}_3$  chains which are linked by  $\text{Si}_2\text{O}_7$  groups. The tetrahedral frame is very open and the water is loosely bound in channels within the framework. The zinc is in tetrahedral coordination with three oxygens and one hydroxyl ion. The mean Zn-O bond is  $1.954\text{\AA}$  (McDonald and Cruickshank, 1967).

Group IV-Complex structures with small cations. This group is characterized by the presence of magnesium and/or manganese, hydroxyl ions instead of water, and layer or slab like structures. All the structures in this group are centric in contrast to those in group III.

In each structure the  $\text{Mn}^{2+}$  or  $\text{Mg}^{2+}$  ions are in regular octahedral coordination despite their smaller size compared to  $\text{Zn}^{2+}$ . In hodgkinsonite  $\text{Zn}_2\text{MnSiO}_4(\text{OH})_2$  (Rentzeperis, 1963) and gerstmannite  $(\text{Mn},\text{Mg})\text{Mg}(\text{OH})_2(\text{ZnSiO}_4)$  (Moore and Araki, 1977a) the Mn,Mg cations are coordinated in octahedrons by the hydroxyl ions and these octahedrons are arranged into brucite like layers. Between these layers are zincosilicate tetrahedral layers or slabs. This layered structure produces a perfect basal cleavage and optical properties similar to the phyllosilicates.

Holdenite  $(\text{Mn},\text{Mg})_6\text{Zn}_3(\text{OH})_8(\text{AsO}_4)_2(\text{SiO}_4)$  (Moore and Araki, 1977b) and mcgovernite  $\text{Mn}_9\text{Mg}_4\text{Zn}_2\text{As}_2\text{Si}_2\text{O}_{17}(\text{OH})_{14}$  (Wuensch, 1960) are very complex structures containing arsenic as an additional tetrahedral cation. Holdenite is composed of

arsen-zincosilicate slabs that sandwich discontinuous islands of Mn,Mg octahedrons in which the cations are surrounded by hydroxyl ions.

The structure of mcgovernite has not been determined primarily because of its platy habit and unusual cell dimensions ( $a=8.22\text{\AA}$ .  $c=205.5\text{\AA}$ ).

A very notable group of exceptions to the tetrahedral coordination of zinc in silicates are the zincian phyllosilicates: hendricksite,  $K(\text{Zn,Mn})_3\text{AlSi}_3\text{O}_{10}(\text{OH})_2$ , (Fron del, 1966), sauconite, and zincsilite (Smol'yaninova, 1961). In each of these minerals zinc is apparently in octahedral sites which are normally occupied by  $\text{Fe}^{2+}$  or  $\text{Mg}^{2+}$ . The large interlayer cation has no effect on the coordination in the octahedral layer and these minerals are clearly members of group IV. These minerals are an exception to the normal balance which exists between zinc and silicon in tetrahedral structures and represent a clear case of structural domination by the aluminosilicate tetrahedral layers. Except for hendricksite which can be synthesized in the laboratory it is not clear whether the zincian phyllosilicates have crystallized directly with zinc in the octahedral sites or whether they are the result of later substitution of zinc in previously existing structures.

#### STRUCTURAL PATTERNS

With the exception of the synthetic pyroxene and

amphibole-like zinc silicates all of the structures described have very large tetrahedral sharing coefficients and are built of two or three dimensional unterminated tetrahedral networks.

$[\text{ZnO}_3]^{4-}$  tetrahedral chains are common in compounds where the Zn/Si ratio is greater than or equal to one. The articulation of the chains differ in each structure and bear little similarity to the  $[\text{SiO}_3]^{2-}$  chains in pyroxenes and pyroxenoids. Zinc-oxygen-zinc bridging angles are on the order of  $115^\circ$  which is considerably smaller than the equivalent angles in silicate chains. In compounds where the Zn/Si ratio is less than unity the  $\text{ZnO}_4$  tetrahedrons are generally isolated.

Cations other than zinc or silicon are generally in irregular coordination in groups I, and III and in regular coordination in groups II, and IV.

The occurrence of hydroxyl ions is restricted to structures where the hydroxyl oxygen atom is not bonded to silicon. Because of the very high tetrahedral sharing of three dimensional tetrahedral networks  $\text{OH}^-$  ions are effectively excluded from these structures with the exception of hemimorphite. Hydroxyl ions are restricted to the layered structures of group IV where tetrahedral sharing is not as great and they can be accommodated in the octahedrons occupied by other cations in a manner similar to the phyllosilicates.

### Acentric Structures

The incidence of acentric and hemimorphic structures is exceptionally high among zinc silicates with approximately 48% of the known structures being acentric and 82% of the acentric structures being hemimorphic.

In the classification discussed, two groups contain predominately acentric structures; group II the wurtzite derivatives and group III the complex structures with large cations.

In the case of zincite (group II) the tetrahedral coordination of zinc requires that it assume either a sphalerite or wurtzite structure. The preference for the wurtzite structure can probably be explained on the basis of the site symmetry available in the two structures. An examination of the Zn-O bond lengths for tetrahedrally coordinated zinc in a large number of structures indicates a consistent inequality in the Zn-O bonds; there is one much shorter bond in  $ZnO_4$  tetrahedrons. This bond inequality is probably related to the covalent character of the Zn-O bond, but because the nature of this bond is not well understood the exact origin of the inequality cannot, at this time, be explained.

The presence of bond asymmetry would lead zinc to favor sites with relatively low symmetry. In wurtzite the zinc atoms are in sites with  $3m$  symmetry and hence the

nonequivalent bond may be accommodated along the unique axis. In the sphalerite structure the zinc atoms are in sites of  $\bar{4}3m$  symmetry which provide no possibility for nonequivalent bonding. Because of these conditions zincite prefers the wurtzite configuration.

In the remaining structures of group II the zinc atoms fall in low symmetry sites on mirror planes, a condition which is consistent with the foregoing conclusions.

The compounds in group III, with one exception, crystallize in acentric space groups and all but one of these are polar. In all cases zinc occurs in sites of low symmetry (usually the general position). Acentric sites exist, however, in centric structures, making it impossible to correlate the occurrence of acentric structures with the need for acentric sites.

The occurrence of polar structures appears to be related in some manner to the nature of the zinc-silicate framework. All the polar structures are based on a three dimensional tetrahedral network in contrast to the nonpolar structures which are frequently layer-like two dimensional tetrahedral networks.

In zinc silicate framework structures there is apparently a balance in bond strengths despite the obvious anisodesmic nature of a Zn-O-Si network. Evidence for the existence of such a balance is observed in the structures of clinohedrite

and junitoite where, despite the presence of equal amounts of zinc and silicon, it is the zinc tetrahedrons that are polymerized and the silicon tetrahedrons which are isolated. This relationship is not what would be expected if the Si-O bond was much stronger than the Zn-O bond as simple bond strength calculations would indicate.

Other zinc bearing tetrahedral structures such as zinc phosphates, arsenates, and sulfates often contain zinc in six-fold coordination as well as four-fold and are uniformly centric. In sulfates, arsenates, and phosphates the bonding is more anisodesmic and the stronger nonzinc metal-oxygen tetrahedral bonds may dominate the structure overriding zinc's ability to form in the preferred tetrahedral coordination.

The occurrence of acentric structures in all but one of the group III compounds indicates that the size of the cations present, in addition to zinc and silicon, affects the structure. The effect of cation size has already been pointed out in group II where the centric phase of  $\text{Na}_2\text{ZnSiO}_4$  does not form because of the cation-cation repulsion in edge sharing tetrahedrons.

The relationship is not as clear for group III compounds. Hardystonite is the only member of this group which is not a polar structure (the structure of esperite has not been determined) and is also the only member which does not contain a three dimensional tetrahedral framework. The existence of

a three dimensional tetrahedral network requires that coordination polyhedrons of the large cations must share their edges with the network. The sharing of faces and edges between one of these polyhedrons and a tetrahedron is impossible because of size. The polyhedral edges must be shared with multiple tetrahedral units. In all of the structures in group III each large cation polyhedron shares some of its edges with pairs of articulated tetrahedrons which are part of the tetrahedral network.

The tetrahedral units are restricted in their arrangement because of the relatively highly charged cation at their center in the case of silicon or large cations in the case of zinc. The geometry of this situation permits only poor packing of tetrahedrons and large cation polyhedrons in centric space groups, and hence acentric structures may be favored. These conditions also result in the irregular coordination of the large cations which is common in group III. Why polar acentric structures result from these conditions rather than nonpolar acentric structures is not clear.

In group I and IV compounds the existence of only tetrahedral sheets and chains give a much greater flexibility and eliminates the packing problems which may lead to acentric structures.

Although existence of a center of symmetry may

facilitate the balancing of forces within the crystal lattice it does not lead to the most efficient packing of irregular coordination polyhedra. Somewhere between the lower energy afforded by the freedom of acentric structures and the need to maintain a short range static equilibrium of interatomic forces lies a balance point which, in most minerals, favors the centric structures. What factors are present in zinc silicates and other acentric structures which favor their formation cannot be exactly determined by geometric analysis and comparison of crystal structures. Only when it is possible to calculate the lattice energy of similar centric and acentric structures will it be possible to explain why the crystal formed with or without a center of symmetry.

### SUMMARY AND CONCLUSIONS

The structure of junitoite, while representing a new tetrahedral framework topology, has features common to many zinc silicates. These features are zinc in tetrahedral coordination, zinc tetrahedrons linked into  $[\text{ZnO}_3]_n^{4n-}$  meta-chains, and an unterminated three dimensional tetrahedral network composed of both zinc and silicon tetrahedrons. Zinc silicates are structurally diverse. Beyond the similarities listed junitoite shows little structural similarity to other zinc silicates.

Based on ionic size considerations alone, zinc which occurs only in the  $\text{Zn}^{2+}$  state should occur in octahedral coordination with oxygen. Octahedral coordination is observed in many compounds but in silicates zinc shows a pronounced preference for tetrahedral coordination. This preference is usually attributed to the covalent nature of the zinc-oxygen bond. An alternate explanation may be that, during crystallization from an aqueous solution, the coordination is determined by the relative size of zinc and  $\text{Si}(\text{OH})_4$  units and not zinc and oxygen.

The polymerization of  $\text{ZnO}_4$  tetrahedrons and the bond length variations in zinc silicates suggests that Zn-O and Si-O are similar and more isodesmic than simple charge and size considerations would indicate.

There are 14 zinc silicate minerals and 11 synthetic zinc silicates with known structures. If the two categories are combined it is possible to divide the zinc silicates into four groups on the basis of chemical and structural similarities. Although a classification based on only 25 structures is bound to appear arbitrary it does serve a useful purpose. The classification allows a systematic discussion of zinc silicates and provides a rapid means for comparison of a very diverse collection of crystal structures. Approximately 40% of the known zinc silicates are hemimorphic a rate well above the 7% value for all inorganic compounds. Although it is not possible to determine why a particular compound crystallizes in a polar structure zinc silicates may offer some insight into the problem. Potential contributing factors are the preference of zinc for low symmetry sites because of nonequivalent bonding, and the packing problems associated with an oversized cation in tetrahedral coordination. The fact that the size of other cations in the structure has a large effect on the polar or nonpolar nature of the structure is a strong indication that geometric considerations are critical in the formation of polar structures in the zinc silicates.

## APPENDIX

OBSERVED AND CALCULATED STRUCTURE FACTORS  
FOR JUNITOITE

H	K	L	FOBS	FCALC
0	0	2	93.6000	78.5227
0	0	4	34.1600	32.5189
0	0	6	58.8400	52.4896
0	0	8	137.4100	122.8696
0	0	10	50.9000	46.3725
0	2	0	27.0400	27.5063
0	2	2	153.7600	152.0697
0	2	4	87.8500	80.0727
0	2	6	125.8700	114.1615
0	2	8	39.1100	38.8769
0	4	0	162.8400	184.6024
0	4	2	50.9500	51.4454
0	4	4	52.4100	49.4264
0	4	6	39.3600	35.0099
0	4	8	97.9900	90.8090
0	6	0	6.6800	5.9495
0	6	2	81.2900	77.1117
0	6	4	59.0600	56.2395
0	6	6	72.6600	65.9214
1	1	1	38.5700	37.6552
1	1	3	66.0200	58.0418
1	1	5	34.6200	32.7024
1	1	7	15.3500	16.0693
1	1	9	14.1300	12.6777
1	2	0	6.9500	3.0439
1	2	2	5.8900	6.8556
1	2	4	13.0200	10.2846
1	2	6	9.2700	5.1333
1	2	8	7.1100	2.5877
1	3	1	36.9500	35.1216
1	3	3	70.9000	63.5873
1	3	5	48.8500	45.1432
1	3	7	25.8700	24.8522
1	3	9	11.1100	5.8826
1	4	0	11.3700	6.9656
1	4	2	13.5000	13.5599
1	4	4	10.6000	7.9929
1	4	6	13.8700	11.2105
1	4	8	6.3700	9.7633
1	5	1	26.3100	22.7236
1	5	3	29.8100	26.3402
1	5	5	18.6400	18.0107
1	5	7	3.5200	6.3967
1	6	0	12.8500	7.5868

H	K	L	FOBS	FCALC
1	6	2	10.7200	11.9800
1	6	4	17.9100	11.6636
1	6	6	11.5700	9.7815
1	7	1	17.1600	17.9103
1	7	3	34.8300	31.6737
2	0	0	72.5300	78.1005
2	0	2	122.6300	127.5191
2	0	4	127.7700	116.8224
2	0	6	94.4000	84.8356
2	0	8	54.6100	52.8276
2	0	10	46.4900	42.9980
2	1	1	5.9400	3.0969
2	1	3	8.2400	3.3969
2	1	5	10.6300	7.2035
2	1	7	4.9800	8.5194
2	1	9	3.3200	10.0827
2	2	0	131.6400	149.7204
2	2	2	106.2200	102.5305
2	2	4	75.3100	72.0393
2	2	6	75.1700	71.6297
2	2	8	70.4200	64.3180
2	3	1	7.9900	4.2251
2	3	3	2.5800	3.8579
2	3	5	10.1300	9.6580
2	3	7	8.5300	9.7229
2	3	9	3.3000	7.0802
2	4	0	59.2900	57.9741
2	4	2	86.6100	85.3790
2	4	4	86.7800	82.1045
2	4	6	67.9500	65.6459
2	4	8	42.5100	41.2766
2	5	1	10.8700	7.3918
2	5	3	7.8800	8.5801
2	5	5	3.2700	7.9458
2	5	7	5.3900	8.6416
2	6	0	79.5100	73.8568
2	6	2	58.7400	57.9402
2	6	4	41.4000	41.9527
2	6	6	43.2000	43.5611
2	7	1	6.5000	8.8510
2	7	3	10.2300	7.5420
3	1	1	73.2200	71.3436
3	1	3	35.4600	34.2243
3	1	5	5.2000	2.0824
3	1	7	53.5900	49.5343
3	1	9	26.2400	25.5320
3	2	0	10.1100	9.4016
3	2	2	9.4100	12.1185
3	2	4	4.6400	3.0332

H	K	L	FOBS	FCALC
3	2	6	6.3300	5.5307
3	2	8	3.2100	1.2431
3	3	1	36.6800	32.9465
3	3	3	7.1300	5.5475
3	3	5	17.6900	16.0593
3	3	7	43.0800	39.6222
3	3	9	15.0900	16.1970
3	4	0	18.6000	16.0686
3	4	2	13.8400	11.2250
3	4	4	8.0600	2.5218
3	4	6	7.1500	6.6217
3	4	8	5.7800	6.6250
3	5	1	50.1600	46.6151
3	5	3	26.3700	25.9077
3	5	5	6.9800	8.1752
3	5	7	39.6400	35.5026
3	6	0	10.0700	13.7269
3	6	2	12.9400	13.1219
3	6	4	9.6800	5.7534
3	7	1	19.5700	16.5835
3	7	3	3.2900	2.8729
4	0	0	86.3900	85.8136
4	0	2	146.2100	160.5429
4	0	4	53.9400	54.9349
4	0	6	92.0100	89.6457
4	0	8	42.4100	37.9780
4	1	1	8.5700	7.4484
4	1	3	2.5200	8.0847
4	1	5	2.7700	4.8190
4	1	7	3.0100	9.1636
4	1	9	8.0700	11.9195
4	2	0	40.9900	41.7434
4	2	2	70.5800	69.4472
4	2	4	172.7300	179.1531
4	2	6	54.4400	56.4514
4	2	8	45.5500	45.1312
4	3	1	4.9800	9.1718
4	3	3	6.5200	15.1467
4	3	5	8.5900	7.1265
4	3	7	6.2600	10.3822
4	4	0	75.1400	71.9940
4	4	2	108.9800	105.3210
4	4	4	30.6500	29.8672
4	4	6	71.4700	70.9608
4	4	8	38.0300	37.2234
4	5	1	4.5900	19.9513
4	5	3	4.1100	15.9365
4	5	5	6.1300	12.9731
4	5	7	8.6900	10.1802

H	K	L	FDBS	FCALC
4	6	0	53.6800	50.4288
4	6	2	34.7900	33.0386
4	6	4	96.5600	88.3141
4	7	1	4.5800	15.0466
5	1	1	57.7100	60.1698
5	1	3	40.2100	44.2560
5	1	5	25.8900	27.5167
5	1	7	39.0900	37.9535
5	1	9	31.8400	32.6682
5	2	0	7.8000	5.3233
5	2	2	7.1800	10.3075
5	2	4	2.7000	7.2735
5	2	6	4.9100	5.0823
5	2	8	6.9600	1.8332
5	3	1	30.9700	29.1181
5	3	3	30.4000	29.6724
5	3	5	28.5200	31.1307
5	3	7	29.4600	29.1889
5	4	0	13.9200	15.2294
5	4	2	11.1900	10.9529
5	4	4	10.9700	6.1809
5	4	6	3.0900	5.8834
5	5	1	46.6300	44.8076
5	5	3	33.9600	31.0692
5	5	5	18.3800	17.9807
5	6	0	12.3700	11.2761
5	6	2	14.4900	14.0649
5	6	4	12.8200	12.0717
5	7	1	19.7400	17.2051
6	0	0	58.2100	55.3952
6	0	2	76.7000	85.6028
6	0	4	112.3700	123.0232
6	0	6	59.5000	64.2802
6	0	8	43.3900	43.5273
6	1	1	6.2200	2.9906
6	1	3	9.8800	8.9170
6	1	5	2.7600	5.7817
6	1	7	4.0300	6.8804
6	1	9	12.9400	10.8626
6	2	0	123.9800	121.8684
6	2	2	91.9000	93.5942
6	2	4	39.7700	41.8987
6	2	6	61.1300	66.0343
6	2	8	56.2300	56.9620
6	3	1	6.8400	6.8472
6	3	3	12.3200	7.2599
6	3	5	6.0700	10.7797
6	3	7	3.3400	8.2170
6	4	0	48.5300	46.7038

H	K	L	FOBS	FCALC
6	4	2	65.3100	61.8233
6	4	4	93.1500	89.7441
6	4	6	50.4700	51.6160
6	5	1	9.9100	9.6292
6	5	3	8.7100	9.4151
6	5	5	5.7400	4.9750
6	6	0	69.8100	65.8740
6	6	2	60.6800	56.0293
6	6	4	26.3300	26.1296
7	1	1	8.8000	3.8120
7	1	3	43.5300	46.9748
7	1	5	20.7600	23.2442
7	1	7	18.1100	17.5435
7	2	0	2.6900	2.0763
7	2	2	2.9300	5.7358
7	2	4	5.1700	6.1046
7	2	6	3.1600	2.5599
7	2	8	3.3900	1.2215
7	3	1	18.9700	20.3450
7	3	3	50.5800	49.2756
7	3	5	31.6300	32.1770
7	3	7	18.8200	22.3005
7	4	0	5.1100	0.5493
7	4	2	12.0500	9.2820
7	4	4	7.7700	6.4894
7	4	6	12.0000	7.8440
7	5	1	10.0500	4.4036
7	5	3	25.7800	25.3434
7	5	5	11.4000	11.4450
7	6	0	12.3500	2.9167
7	6	2	11.4500	10.3569
8	0	0	159.9000	175.3870
8	0	2	63.7600	68.7789
8	0	4	51.7500	57.1729
8	0	6	43.0900	45.4590
8	0	8	83.2500	85.2503
8	1	1	9.1000	4.7640
8	1	3	10.0600	7.6306
8	1	5	9.0000	11.5330
8	1	7	5.8900	9.0205
8	2	0	47.6100	43.7715
8	2	2	98.8300	101.4938
8	2	4	36.2000	40.6560
8	2	6	76.8900	82.4913
8	2	8	38.0400	39.3354
8	3	1	7.1000	8.5323
8	3	3	7.9200	8.7817
8	3	5	3.1500	14.1330
8	3	7	6.7200	13.6674

H	K	L	FOBS	FCALC
8	4	0	121.4200	115.6422
8	4	2	46.9700	46.3057
8	4	4	53.8500	53.4800
8	4	6	32.5800	32.1467
8	5	1	8.5100	14.0633
8	5	3	6.4500	11.0858
8	5	5	3.8700	15.2173
8	6	1	3.2700	0.0000
9	1	1	26.5300	31.3378
9	1	3	35.4500	40.4970
9	1	5	28.2300	31.6895
9	1	7	18.0500	16.9398
9	2	0	7.5100	1.3564
9	2	2	3.0000	4.6671
9	2	4	4.0900	7.4126
9	2	6	4.2800	5.4738
9	3	1	28.2200	26.9561
9	3	3	44.5300	44.6115
9	3	5	33.4700	37.7005
9	3	7	19.2900	21.0785
9	4	0	4.4000	10.0502
9	4	2	8.6000	10.6696
9	4	4	10.5000	6.3827
9	4	6	3.5600	9.7164
9	5	1	24.4000	22.3277
9	5	3	25.5500	23.8452
10	0	0	19.7900	17.7063
10	0	2	69.5300	78.5391
10	0	4	71.2300	79.6579
10	0	6	59.0100	64.1104
10	1	1	10.4400	9.0241
10	1	3	5.4000	4.4769
10	1	5	6.5500	7.9240
10	1	7	10.6200	10.9296
10	2	0	116.1500	115.8328
10	2	2	48.3200	51.8993
10	2	4	35.0400	36.8205
10	2	6	35.4500	37.1566
10	3	1	11.1300	7.5591
10	3	3	7.1300	6.0282
10	3	5	4.8300	11.5905
10	4	0	17.0200	15.7442
10	4	2	63.8100	60.6354
10	4	4	59.7700	62.6492
10	5	1	9.0100	10.5517
10	5	3	3.5500	8.7574
11	1	1	22.3000	26.9804
11	1	3	15.6300	19.7759
11	1	5	8.8600	7.9390

H	K	L	F03S	FCALC
11	2	0	6.9600	2.9669
11	2	2	5.2600	3.9697
11	2	4	3.8100	1.2844
11	2	6	3.5400	2.1059
11	3	1	13.7100	13.8589
11	3	3	10.2700	8.1693
11	3	5	6.4800	7.6652
11	4	0	11.3900	4.5974
11	4	2	3.5800	5.4196
11	4	4	3.4900	2.5250
11	5	1	28.6900	26.0261
12	0	0	31.4500	33.8508
12	0	2	69.1300	79.5153
12	0	4	37.2100	37.2888
12	0	6	51.8600	58.4528
12	1	1	9.0200	8.4273
12	1	3	5.1800	8.7340
12	1	5	10.0900	6.8828
12	2	0	49.4600	48.6124
12	2	2	40.3400	43.3726
12	2	4	79.1700	89.1515
12	3	1	10.4800	9.8427
12	3	3	4.0200	11.4033
12	4	0	32.8500	33.9981
12	4	2	63.9000	63.6018
13	1	1	31.5100	37.9470
13	1	3	15.9400	16.2533
13	2	0	3.3100	3.8535
13	2	2	3.3000	6.0702
13	2	4	3.3400	4.9372
13	3	1	27.1600	27.3646
14	0	0	32.9500	32.5549
14	0	2	32.7800	34.5283
14	1	1	4.9500	6.8450
14	1	3	8.4500	10.9043
14	2	0	56.1800	57.3654
14	2	2	49.0900	56.1685

## REFERENCES

- Abrahams, S.C. and J.L. Bernstein (1969) Remeasurement of the structure of hexagonal ZnO. *Acta Crystallogr.*, B25, 1233-1236.
- Ahmed, F.R., S.R. Hall, M.E. Pippy, and C.P. Saunderson (1967) NRC Crystallographic programs for the IBM/360 system. Natl. Res. Council, Ottawa, Canada.
- Bauer, W.H. (1970) Bond length variations and distorted coordination polyhedra in inorganic crystals. *Trans. Am. Crystallographic Assoc.*, 6, 129-155.
- \_\_\_\_\_ (1971) The prediction of bond length variations in silicon-oxygen bonds. *Am. Mineral.*, 56, 1573-1599.
- Belokoneva, E.L., Y.K. Egorov-Tismenko, M.A. Simonov, and N.V. Belov (1970) Crystal structure of zinc chkalovite  $\text{Na}_2\text{Zn}(\text{Si}_2\text{O}_6)$ . *Kristallografiya*, 14, 1060-1062. (transl. *Soviet Physics-Crystallography*, 14, 918-919).
- Berner, R.A. (1971) Principles of Chemical Sedimentology, McGraw-Hill, New York
- Brehler, B. (1969) Zinc. In K.H. Wedepohl, Ed., Handbook of Geochemistry, p. 30A-1 to 30A-10. Springer-Verlag, Berlin.
- Brown, I.D. (1977) Predicting bond lengths in inorganic crystals. *Acta Crystallogr.*, B33, 1305-1310.
- Busing, W.R. and H.A. Levy (1957) Neutron diffraction study of calcium hydroxide. *J. Chemical Physics*, 26, 563-567.
- \_\_\_\_\_, K.O. Martin, and H.A. Levy (1962) OFRLS, a Fortran crystallographic least-squares refinement program. U.S. Natl. Tech. Inf. Serv., ORNL-TM-305.
- Cornfield, P.W.R., R.J. Doedens, and J.A. Ibers (1967) Studies of metal-nitrogen multiple bonds. I. The crystal and molecular structure of nitridoichlorotris (diethylphenylphosphine) rhenium (V). *Inorganic Chem.* 6, 197-204.
- Cruickshank, D.W.J. (1961) The role of 3d-orbitals in  $\pi$ -bonds between (a) silicon, phosphorus, sulphur, or chlorine and (b) oxygen or nitrogen. *J. Chem. Soc.*, 1961, 5486-5504.

- de Meulenaer, J. and H. Tompa (1965) The absorption correction in crystal structure analysis. *Acta Crystallogr.*, 19, 1014-1018.
- Fron del, C. and J. Ito (1966) Hendricksite, a new species of mica. *Am. Mineral.*, 51, 1107-1123.
- Hang, C., M. A. Simonov, and N. V. Belov (1970) Crystal structures of willemite  $Zn_2SiO_4$  and its germanium analog  $Zn_2GeO_4$ . *Kristallog.*, 15, 457-460. (transl. Soviet Physics-Crystallography, 15, 387-388).
- Heese, K. F., F. Liebau, and H. Bohm (1977) Disodium zinc-silicate,  $Na_2ZnSi_3O_8$ . *Acta Crystallogr.*, B33, 133-1337.
- International Tables for X-ray Crystallography. vol 4, (1976) The Kynoch Press, Birmingham, England.
- Ito, J. (1968) Synthesis of some lead calcium zinc silicates. *Am. Mineral.*, 53, 231-240.
- Louisnathan, S. J. (1969) Refinement of the crystal structure of hardystonite,  $Ca_2ZnSi_2O_7$ . *Z. Kristallogr.*, 130, 427-437.
- McDonald, W. S. and D. W. J. Cruickshank (1967) Refinement of the structure of hemimorphite. *Z. Kristallogr.*, 124, 180-191.
- Marumo, F. and Y. Syono (1971) The crystal structure of  $Zn_2SiO_4$ -II, a high pressure phase of willemite. *Acta Crystallogr.*, B27, 1868-1870.
- MeGaw, H. D. (1968) A simple theory of the off-centre displacement of cations in octahedral environments. *Acta Crystallogr.*, B24, 149-153.
- Moore, P. B. and P. H. Ribbe (1965) A study of "calcium-larsenite" renamed esperite. *Am. Mineral.*, 50, 1170-1178.
- \_\_\_\_\_ and T. Araki (1977a) Gerstmannite, a new zinc silicate mineral and a novel cubic close-packed oxide structure. *Am. Mineral.*, 62, 51-59.
- \_\_\_\_\_, \_\_\_\_\_ (1977b) Holdenite, a novel cubic close-packed structure. *Am. Mineral.*, 62, 513-521.

- Morimoto, N., S. Akimoto, K., Koto, and M. Tokonami (1969) Modified spinel, beta-manganous orthogermanate: stability and crystal structure. *Science*, 165, 586-588.
- \_\_\_\_\_, Y. Nakajima, Y. Syono, S. Akimoto, and Y. Matsui (1975) Crystal structures of pyroxene-type  $ZnSiO_3$  and  $ZnMgSi_2O_6$ . *Acta Crystallogr.*, B32, 1041-1049.
- Pauling, L. (1960) The Nature of the Chemical Bond, 3rd Ed. Cornell University Press, Ithaca, N.Y.
- Perry, D. V. (1969) Skarn genesis at the Christmas Mine, Gila county, Arizona. *Econ. Geol.*, 64, 255-270.
- Prewitt, C., T. E. Kirchner, and A. Preisinger (1967) Crystal structure of larsentite  $PbZnSiO_4$ . *Z. Kristallogr.*, 124, 115-130.
- Rentzeperis, P. J. (1963) The crystal structure of hodgkinsonite  $Zn_2Mn(OH)_2SiO_4$ . *Z. Kristallogr.*, 119, 117-138.
- Ross, C. S. (1946) Sauconite-a clay mineral of the montmorillonite group. *Am. Mineral.* 31, 411-424.
- Rosler, U. (1969) Energy bands of hexagonal II-VI semiconductors. *Physical Review*, 184, 733-738.
- Smol'yaninova, N.N., V. A. Moleva, and N. I. Organova (1961) Zincsilite. *Am. Mineral.* 46, 242-
- Syono, Y., S. Akimoto, and Y. Matsui (1971) High pressure transformations in zinc silicates. *J. of Solid State Chem.*, 3, 369-380.
- Tossell, J. A. (1975) The electronic structures of silicon, aluminum, and magnesium in tetrahedral coordination with oxygen from SCF-Xa Mo calculations. *J. Amer. Chem. Soc.*, 97, 4840-4844.
- Venetopulos, C. C. and P. J. Rentzeperis (1976) Redetermination of the crystal structure of clinohedrite,  $CaZnSiO_4 \cdot H_2O$ . *Z. Kristallogr.*, 144, 377-392.
- West, A. R. (1975) Crystal chemistry of some tetrahedral oxides. *Z. Kristallogr.*, 141, 422-436.

- Williams, S. A. (1976) Junitoite, a new hydrated calcium zinc silicate from Christmas, Arizona. *Am. Mineral.*, 61, 1255-1258.
- Wuensch, B. J. (1960) The crystallography of mcgovernite, a complex arsenosilicate. *Am. Mineral.*, 45, 937-945.
- Zoltai, T. (1960) Classification of silicates and other minerals with tetrahedral structures. *Am. Mineral.*, 45, 960-973.